IFAC

INTERNATIONAL FEDERATION
OF AUTOMATIC CONTROL

WARSZAWA 1969

Fluidics

Fourth Congress of the International
Federation of Automatic Control
Warszawa 16–21 June 1969

TECHNICAL
SESSION
22

Organized by
Naczelna Organizacja Techniczna w Polsce

INTERNATIONAL FEDERATION OF AUTOMATIC CONTROL

Fluidics

TECHNICAL SESSION No 22

FOURTH CONGRESS OF THE INTERNATIONAL
FEDERATION OF AUTOMATIC CONTROL
WARSZAWA 16 – 21 JUNE 1969

Organized by
Naczelna Organizacja Techniczna w Polsce

Contents

Wydawnictwa Czasopism Technicznych NOT - Polska

Zakład Poligraficzny WCT NOT. Zam. 102/69.

OPTIMIZATION OF THE PNEUMATIC INTEGRATED CIRCUITS WITH JET DEVIATION, FOR AUTOMATIC COMPUTERS AND CONTROLS

by the research team F.P.Ms. - C.R.I.F. - S.A.B.C.A. *

* The research team F.P.Ms. - C.R.I.F. - S.A.B.C.A. includes :

Professor Raoul MOLLE, Research Manager ; MM. Jean HUCHANT, Research Engineer at S.A.B.C.A. ; Pierre BERNIMOLIN, Research Engineer at C.R.I.F. ; Roger LAURENT and Marius CALERS, Engineers at the Design Office of S.A.B.C.A.

F.P.Ms. : Faculté Polytechnique of Mons - Belgium.

C.R.I.F. : Centre de Recherches Scientifiques et Techniques de l'Industrie des Fabrications Métalliques.

S.A.B.C.A. : Société Anonyme Belge de Constructions Aéronautiques.

These researches are effected in the Laboratory of Technology, Metrology and Mechanical Engineering of the Faculté Polytechnique de Mons, with the material and financial assistance of I.R.S.I.A. (Institut pour l'encouragement de la Recherche Scientifique dans l'Industrie et l'Agriculture), C.R.I.F. and S.A.B.C.A.

SUMMARY AND INTRODUCTION

The realization of integrated pneumatic circuits for process automatisation, from models of logical components with jet deviation, sets a problem of cost and behaviour optimization of these circuits.
This problem can be approached by means of electrical homologies using R-C circuits, operational amplifiers and, in case of components with COANDA effect, of Schmitt triggers.

The present study shows how to choose the electrical values of the circuit parameters, to obtain a dynamic behaviour analogous to this of the equivalent pneumatic circuit.

The inverse reasoning allows to fix the parameters of a pneumatic circuit, homologous of this of an electronic circuit, and to predict its behaviour.

The pursued objective is the creation and the preliminary study of homologous electronic circuits, so as to optimize the choice, the relative position and the interconnection modes of the diverse fluidic components of the future integrated pneumatic circuits.

To explain our method of electric simulation of pneumatic circuits, the easiest way is to take an example.

We shall simulate the circuit of fig. 1, realizing an amplifier composed of 2 elements with jets deviation P1 and P2, the second one acting as load for the first one.

We first will define the characteristics of the pneumatic circuit, which will give us the basic homology coefficients.
To realize the electric circuit, a minimum of measures must indeed be effectuated.

STATIC AND DYNAMIC CHARACTERISTICS OF THE PNEUMATIC CIRCUIT

The static outlet characteristic (fig. 2) gives the outlet flow of the first element Q_Y in terms of the pressure drop in this element $P_{X_1} - P_{Y_{11}}$ and of the difference of the inlet pressures ΔP_Y .
This characteristic also contains the load lines corresponding to circuit $Y_{11}.Y_{12}$.
These lines are given for different values of P_{X_1}.
By choosing the operating point at rest A, corresponding to P_{X_1} = 250 mm Hg and $\Delta P_Y = 0$, one can calculate static coefficients.
These can be assimilated to electric resistances and contain thus only a real part, i.e. no depending on the frequency.
We define them by the relation $R = \Delta P/Q = \Delta P/Q_v.\rho$ to obtain the homologous of the electric resistance R = U/I ; then we utilize the following pneumo-electrical homology :

$\Delta P = U$: pressure drop = voltage drop

$Q = I$: massic flow : current strength

Let us note $Q = Q_v.\rho$: massic flow = volumetric flow x mass density.

$$\rho = \frac{P}{r.T}$$ mass density

$r = 287\ m^2/s^2.\ ^\circ K$.

T = temperature in °K

In the considered case, we define :

$$R_y = \left[\frac{\delta(P_x - P_y)}{\delta Q_y}\right]_{\Delta P_y = C^{te}}$$ outlet resistance

$$R = \left[\frac{\delta(P_x - P_y)}{\delta Q_y}\right]_{P_x = C^{te}}$$ load resistance

We ascertain that those resistances are nothing else than the angular coefficients of the outlet and load characteristics of figure 2.

We can thus calculate them about the point of rest A, as far as the characteristics are linear or linearized.

We obtain here :

$$R_y = \frac{108\ mm\ Hg}{2\ cm^3/s.\rho} = 1,42.10^{11}\ 1/m.s$$

$$R = \frac{39,5\ mm\ Hg}{2\ cm^3/s.\rho} = 1,04.10^{10}\ 1/m.s$$

$$\rho = \frac{32\ mm\ Hg}{287\ m^2/s^2.°K.293\ °K}$$

From the outlet characteristics of figure 2, we also define an amplification coefficient in pressure between inlet and outlet :

$$K_p = \left[\frac{\delta(P_x - P_y)}{\delta(\Delta P_y)}\right]_{\Delta_y = C^{te}}$$

$$= \frac{30\ mm\ Hg}{50\ mm\ water} \text{ for } \Delta P_y > 0$$

$$= \frac{19,4\ mm\ Hg}{50mm\ Water} \text{ for } \Delta P_y < 0$$

$K_{p.moyen} = 27,4$

The static inlet characteristic of figure 3 gives the inlet flow in terms of the inlet pressure . It allows us to define an inlet resistance :

$$R_y = \frac{\partial P_y}{\partial Q_y} = 1,85.10^{10}\ 1/m.s$$

Concerning dynamical characteristics, we can record the impulsional, indexial and frequencial responses which allow us to calculate the pneumatic capacity that we define by $C = \frac{\int Q.dt}{\Delta P}$, as in electricity, $C = \frac{\int I dt}{U}$.
The value of a capacity essentially depending on the frequency, we must necessarily measure it from a dynamical characteristic.

The easiest way to determine the capacity is, under the circumstances, to utilize the indexial response which gives us directly $\int Q.dt$ or ΔP .
The inlet impulse is given by a triggered bistable element, and we record the responses in flow and in pressure.

For an example, to measure the outlet and load capacities, we apply a pressure signal from 250 mm water up to practically 0 mm water in y_{11} and we record in y_{11}, y_{22} (fig. 1) a response in discharge varying from 12 cm^3/s to 3 cm^3/s (fig. 2).
We shall see later on that the plotted pneumatic Bode diagram corresponds to a sinusoidal wave varying between 250 and 150 mm water in .
Let us thus limit the indexial response to these two values, which corresponds to a response in flow varying between 12 cm^3/s and 6 cm^3/s.

The enlargement of the oscillographic recording at the profiles projector allows the planimetering and gives $\int Q dt = 6{,}05.10^{-10}$ kg masse
On the other hand, the response in pressure varies between 39,5 and 5 mm Hg.

We thus obtain :
$$C_y + C = \frac{6{,}05\,10^{-10}\ kg}{34{,}5\ mm\ Hg} = 1{,}32.10^{-13}\ m.s^2$$

The inlet capacity C_y ranges about 10^{-15} ms, which is negligible towards the further one.
We take indeed directly place at the inlet of element P1.

PROPERLY SO CALLED ELECTRICAL HOMOLOGY

After having measured some characteristic coefficients of the circuit, let us establish its electrical homologous.
Several studies of the internal working mechanism of the amplifier with jets deviation, allow to replace it by the principle diagram of figure 4.

$Z_i = R_i + \frac{1}{j\omega C_i}$ are pneumatic impedances wherein intervene the pneumatic capacities and resistances defined above.
Let us note that Z_x is the impedance of the power feeding circuit.

If we express the pressure drop in the left branch, then in the right branch of the amplifier, and if we calculate the difference between these two terms, we obtain an equality which is translated by the equivalent electrical diagram of figure 5.

We naturally use the same pneumo-electrical homology as the abovementioned one.

The values of the pneumatic capacities and resistances calculated above, are directly utilizable by expressing the following equivalence : $\frac{1}{m.s} = 1\,\Omega$, $1\,m.s^2 = 1\,F$

Unfortunately, this way of proceeding does only lead to electrical greatnesses which are not easy to realize. We may fortunately multiply the resistances by a constant factor (10^{-5}) and the capacities by the inverse of this factor (10^{5}) to keep a circuit equivalent to the first one and the elements values of which are : $R_y = 185\,k\Omega$, $R_Y = 1{,}42\,M\Omega$, $R = 10^4\,\Omega$

$C_{Y+C} = 0{,}0132\,\mu F$, $C = 0{,}1\,\mu F$

Let us note that $2K_p$ is an electronic operational amplifier of $2K_p = 54{,}8$

The Bode diagram of this electric circuit, homologous of the pneumatic circuit, is drawed on figure 6.

We plot it by driving the circuit with a generator of sinusoidal functions and recording the inlet and outlet signals by means of a memoscope.

VERIFICATION OF THE METHOD VALIDITY

To verify the validity of the method, the easiest way is to compare the pneumatic Bode diagram to the Bode diagram of the electric circuit, plotted above.

To this end, we utilize a generator of pneumatic sinusoidal functions the principle of which is given on figure 7.

An eccentric wheel turns in front of a nozzle and generates a sinusoidal pressure P2, as far as the dimensions of the set are well chosen.

This sinusoidal wave is deformed by a high frequency noise that we eliminate by a pneumatic low-pass filter realized by a capacity placed between the P2 pressure nozzle and the inlet of the element.

So we obtain a purified sinusoidal inlet signal which allows us to plot easily the pneumatic Bode diagram by means of pressure captors and of a memoscope.

Let us note that the amplitude of the inlet signal is maintained constant in function of the frequency, by having the internal capacity of the under pressure nozzle P2 varied.

In the considered example, the purified sinusoidal signal $P_{y\,11}$ is 100 mm water worth from point to point (150 to 250 mm water).

The other adjustments are : $P_{32.1} = 200\,mm\ water$, $P_{x1} = P_{x2} = 250\,mm\ Hg$

$C_{v+C} = 1{,}5\,cm^3$

The pneumatic Bode diagram we have plotted is drawed on figure 6.
We ascertain that this latest one is practically similar to the electric Bode diagram.
The amplitude difference is of the range of 1 dB and the phase variation of the range of 20° . The cut-off frequency is of about 25 Hz.

We deduce that the used homology is sufficiently valid.

CONSEQUENCES

This homology method allows us to predetermine the indexial, impulsional and frequencial responses of a pneumatic circuit, as far as we dispose of some basic measures.

We dispose thus of an extremely precious tool, pleasant to utilize, which allows us to apply to a pneumatic circuit the numerous information placed at our dispos by the electrical theories.
For an example, we can determine the responses of our pneumatic circuit by electrical measures, which are, as everybody knows, much easier.

We also can, by utilizing the theory of electric circuits, determine the transfe function of our electric circuit and deduce of it the homologous pneumatic circu

If we want to study the behaviour of an amplifier with several stages, including some filters, delay lines, diodes ... it is sufficient to put in cascades sever circuits of the same kind as this of figure 5.

This method also allows to optimize an element or circuit by varying electric elements, which is clearly easier than modifying a pneumatic circuit board asse bly.

Let us also note, to be complete, that the simulation of the bistables and mono stables needs electronic flip-flops instead of operational amplifiers.

To build and optimize the integrated circuit responding to any problem, it is sufficient to know the simulation of the several basic elements of the circuits and to study the best way to connect them.

This brings us back to the study of an electric mesh circuit which, if it corr tly works, certifies the working of the graved pneumatic circuit.

It is thus logical to take up the preliminary designs of the integrated pneuma circuits by means of electronic simulations.
This new method must allow to attain more rapidly and surely the optimal form, on measure, of the complex and integrated circuits of any pneumatic automatisa

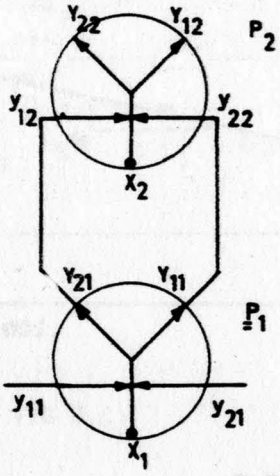
Y_{22}
Y_{12}
P_2
y_{12}
y_{22}
X_2
Y_{21}
Y_{11}
P_1
y_{11}
y_{21}
X_1

FIG. 1

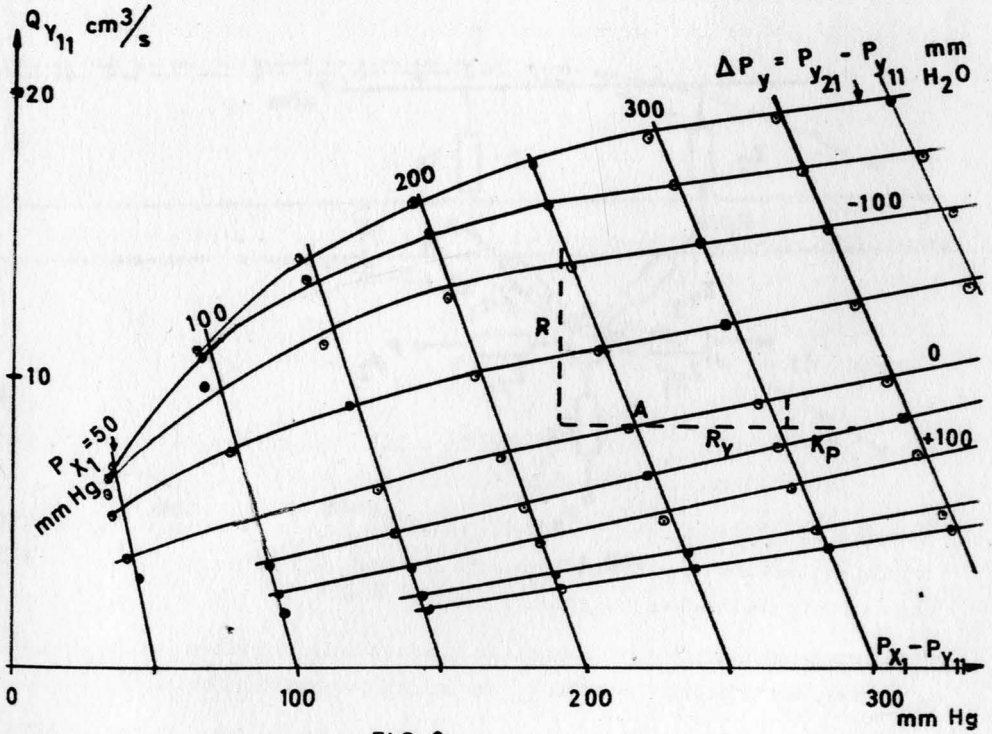
$Q_{Y_{11}}$ cm³/s
20
10
$\Delta P_y = P_{y_{21}} - P_{y_{11}}$ mm H_2O
300
200
100
-100
0
+100
R
A
R_y
R_P
$P_{X_1} = 50$ mm Hg
$P_{X_1} - P_{Y_{11}}$
0
100
200
300
mm Hg

FIG. 2

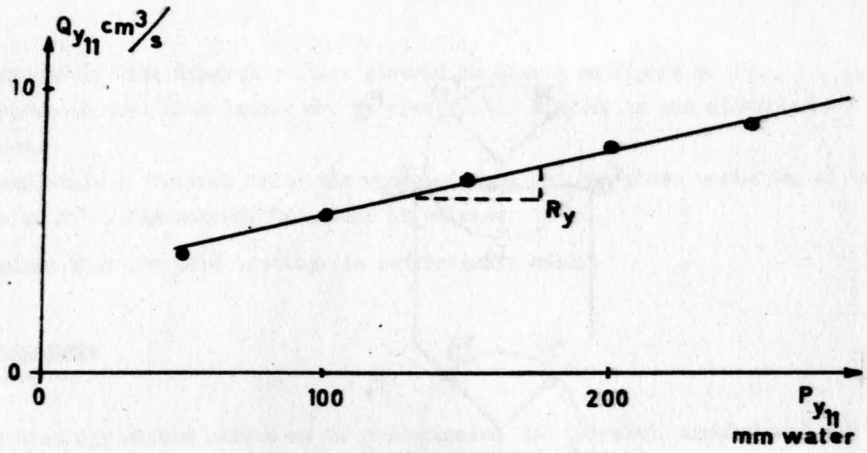
$Q_{y_{11}}$ cm³/s
10
0
0
100
200
$P_{y_{11}}$
mm water
R_y

FIG. 3

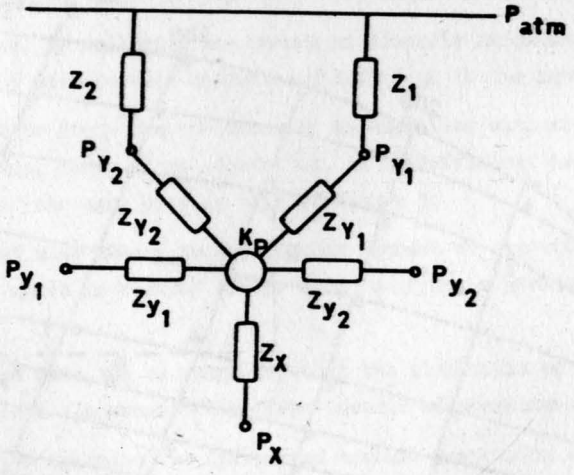
P_{atm}
Z_2
Z_1
P_{Y_2}
P_{Y_1}
Z_{Y_2}
K_P
Z_{Y_1}
P_{y_1}
P_{y_2}
Z_{y_1}
Z_{y_2}
Z_X
P_X

FIG. 4

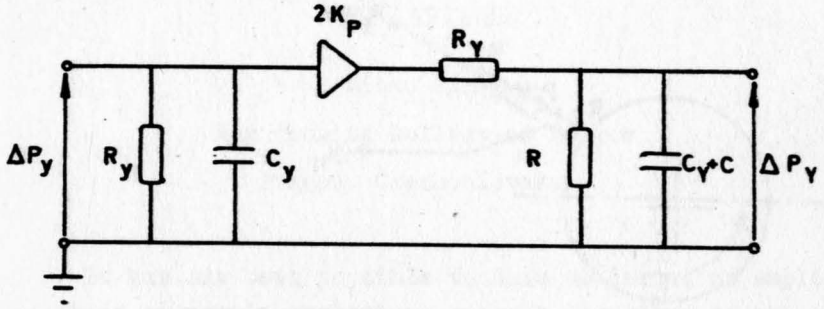

FIG. 5

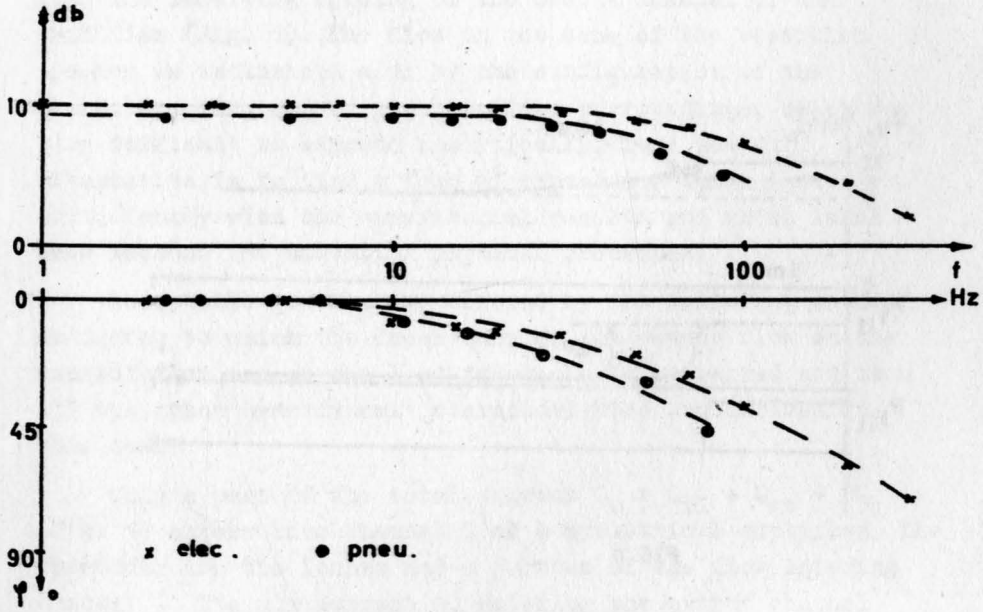

FIG. 6

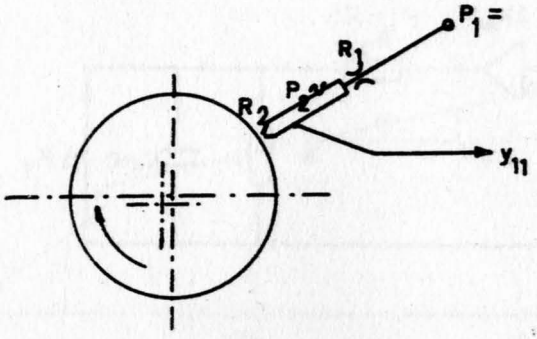

FIG. 7

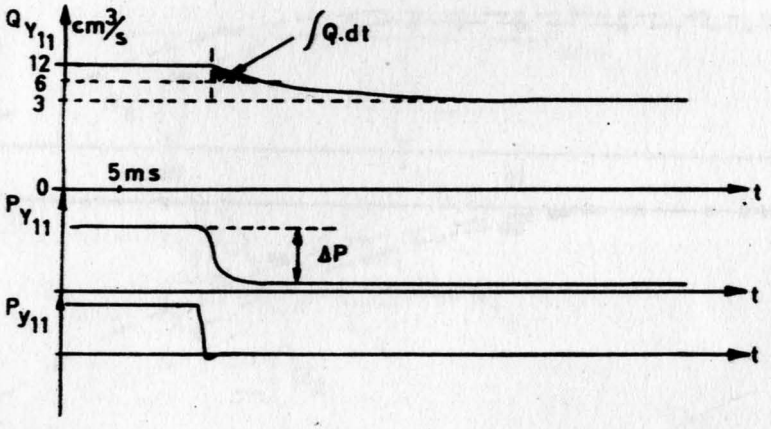

FIG. 8

ON THE THEORY OF PROPORTIONAL FLOW AMPLIFIERS

Milan BALDA

Engineering College of Prague

Prague, Czechoslovakia

It has not been possible to date to derive an amplification equation by purely analytical methods according to which it would be possible to calculate the dynamic characteristics (dependence of the output flow on the controlling current and on the load impedance). The reason for this is the complexity of the hydrodynamic conditions especially at the input of the deflected and whirled up free turbulent current into the receiving opening of the output channel of the amplifier (Fig. 1). The flow in the zone of the reception opening is influenced also by the configuration of the channel opening and by its immediate surroundings, which is very difficult to express analytically. Thus the only alternative is to find a form of expression which agrees sufficiently with the experimental results and which takes into account the essential physical processes.

Acceptable results are offered by the following method, according to which the dependency of the output flow on the control flow and on the load impedance is expressed and then all the other hydrodynamic characteristics are derived on this basis.

Only a part of the total current $Q_k + Q_{r1} + Q_{rz} + 2Q_b$ (Fig. 1) enters into channel 1 of a symmetrical amplifier, the remainder are the losses and a portion of the flow entering channel 2. The air current Q_1 entering the output channel is split up into the output current Q_{v1} and the loss current Q_{z1} which depends on the load impedance.

The Bernoulli's equation can be written for the input part a-b of the output channel. As the current Q_1 enters the space at a certain positive pressure which depends on the p_{v1}, we get

$$\tfrac{1}{2}\varrho c_1^2 + k_n p_{v1} = \tfrac{1}{2}\varrho c_{v1}^2 + p_{v1}$$

wherein the velocity c_1 as the mean velocity in the section F_a is assumed to be

$$c_1 = Q_1/F_a$$

and by analogy

$$c_{v1} = Q_{v1}/F_b$$

For $F_a = F_b$ and $\varrho Q_k^2 / 2p_k = (\alpha F_k)^2$ the Bernoulli's equation can be written in the following dimensionless form:

$$\left(\frac{\alpha F_k}{F_a}\right)^2 \left(\frac{Q_1}{Q_k}\right)^2 + k_n \frac{p_{v1}}{p_k} = \left(\frac{\alpha F_k}{F_a}\right)^2 \left(\frac{Q_{v1}}{Q_k}\right)^2 + \frac{p_{v1}}{p_k} \qquad (1)$$

The pressure in the output channel 1 depends on the load impedance

$$p_{v1} = Q_{v1} Z_{v1}$$

or

$$\frac{p_{v1}}{p_k} = \frac{Q_k}{p_k} R_i \frac{Q_{v1}}{Q_k} \frac{Z_{v1}}{R_i} \qquad (2)$$

wherein R_i represents the inner resistance.

The dependence of current Q_1 on the control current Q_r can be derived in the following form: the direction of the resulting current is given by the vector sum of the momentum of the power current Q_k and of the control current Q_r

$$\gamma = \omega c \operatorname{tg} \frac{(Hr/Hk)\sin\beta}{1 + (Hr/Hk)\cos\beta}$$

and for $\gamma = 90^{o}$ (as is usually the case) $Q_{r1} / Q_k = (tg\gamma \cdot F_r / F_k)^{\frac{1}{2}}$

where $H_r = F_r c_r^2 \varrho$ ... throughput momentum of the control current [N]

and $H_k = F_k c_k^2 \varrho$ ... throughput momentum of the power current [N]

If there is a linear relationship between Q_1 and Q_{r1}, we get

$$\left.\frac{Q_{r1}}{Q_k}\right|_{Q_1=0} = \frac{Q_{r1max}}{Q_k} = \left[F_r / F_k \cdot tg\,\gamma_{max}\right]^{\frac{1}{2}} = \frac{1}{k_3}$$

for the limit value of Q_{r1}, where k_3 is a construction constant. For the conventional types of proportional amplifiers ($\gamma_{max} \cong 9^{o}30$ and $F_r/F_k = 1.5$) $k_3 = 2$.

Thus $$Q_1 / Q_k = k_1 (1 - k_3 Q_{r1} / Q_k) \qquad (3)$$

where k_1 indicates the maximum output current for the case where $Q_{r1} = 0$ and $Z_{v1} = 0$:

$$k_1 = Q_1 / Q_k \Big|_{Q_{r1}=0,\ Z_{v1}=0} = k_3 (0.5\, Q_b / Q_k) \cong Q_{v1} / Q_k \Big|_{Q_{r1}=0,\ Z_{v1}=0}$$

The current Q_b is also referred to as bias. In most cases $Q_b = 0$ and in this case $k_1 = 0.70 \ldots 0.75$ (so called flow recovery).

The following expression can be introduced as the internal resistance

$$R_i = p_k / Q_{v1} \Big|_{Q_{r1}=0,\ Z_{v1}=0} \qquad (4)$$

We obtain the following relation from the equations (1), (2), and (3), and (4):

$$\left(\alpha\frac{F_K}{F_a}\right)^2 k_1^3\left(1-k_3\frac{Q_{r1}}{Q_K}\right)^2=\left(\alpha\frac{F_K}{F_a}\right)^2\left(\frac{Q_{r1}}{Q_K}\right)^2 k_1+2\frac{Q_{v1}}{Q_K}\cdot\frac{Z_{v1}}{R_i}(1-k_n) \qquad (5)$$

From which the constant k_4 is to be eliminated. From equations (1) and (3) for $Q_{r1} = 0$ and $Z_{v1} = \infty$ we obtain

$$k_4 = 1-\frac{k_1^2}{k_2}\left(\alpha\frac{F_K}{F_a}\right)^2$$

where

$$k_2 = p_{v1}/p_K\Big|_{Q_{r1}=0,\ Z_{v1}=\infty}$$

is termed as pressure recovery and represents a further characteristic magnitude of the amplifier. With the coventional types $k_2 = 0.40...0.45$

We finally obtain a planar symmetrical proportional amplifier as an equation

$$\frac{Q_{vj}}{Q_K} = \frac{k_1}{2k_2}\left[\sqrt{\left(\frac{Z_{vj}}{R_i}\right)^2+\left(2k_2\right)^2\left(1-k_3\frac{Q_{rj}}{Q_K}\right)^2}-\frac{Z_{vj}}{R_i}\right] \qquad (6)$$

where $j = 1,2$

$$k_1 = Q_{vj} / Q_K \Big|_{Q_{rj}=0,\ Z_{vj}=0}$$

$$k_2 = p_{vj} / p_K \Big|_{Q_{rj}=0,\ Z_{vj}=\infty}$$

$$k_3 = \left[(F_r / F_K) \cdot \operatorname{tg} \gamma_{max}\right]^{-\frac{1}{2}}$$

$$R_i = p_K / Q_{vj} \Big|_{Q_{rj}=0,\ Z_{vj}=0}$$

The load characteristic is calculated from the equation

$$\frac{p_{vj}}{p_K} = \frac{1}{k_1} \frac{Q_{vj}}{Q_K} \frac{Z_{vj}}{R_i} \qquad (7)$$

The load graph of the CORNING type FD-2511-3-1321 amplifier has been calculated as an example and compared with the data published in the catalogue. We can gather from Fig. 2 that the calculated values (market with a cross) are in good agreement with the experimental data.

Listing of the notations used in the foregoing

A	amplification	/-/
c	velocity	/ms^{-1}/
F	section	/m^2/
H	throughput momentum	/N/
k	constant of proportionality	/-/
p	pressure	/Nm^{-2}/
Q	throughput quantity, flow	/m^3s^{-1}/
R	resistance	/Nsm^{-5}/
Z	impedance	/Nsm^{-5}/
α	throughput index	/-/
β	angles between the axes of the power and control nozzle	/°/
γ	deflection angle of the flow	/°/
ϱ	specific gravity	/kgm^{-3}/

The indices signify:

b	bias
k	feed
r	control
v	output
z	loss
1, 2	position or order

Literature

/1/ Balda M.: Statische Kennlinien des pneumatischen Verstärkers mit freier turbulenter Strömung. (in Automatizace 8 /1966/, Issue No. 9, p. 233-238, 12 Fig.) (in tschechisch)

/2/ Balda M.: Theorie der pneumatischen nach dem Interaktionsprinzip arbeitenden Strömungsverstärker. Acta Polytechnica CVUT, II, No. 2 (1967), p. 59-68, 7 Fig. (in tschechisch)

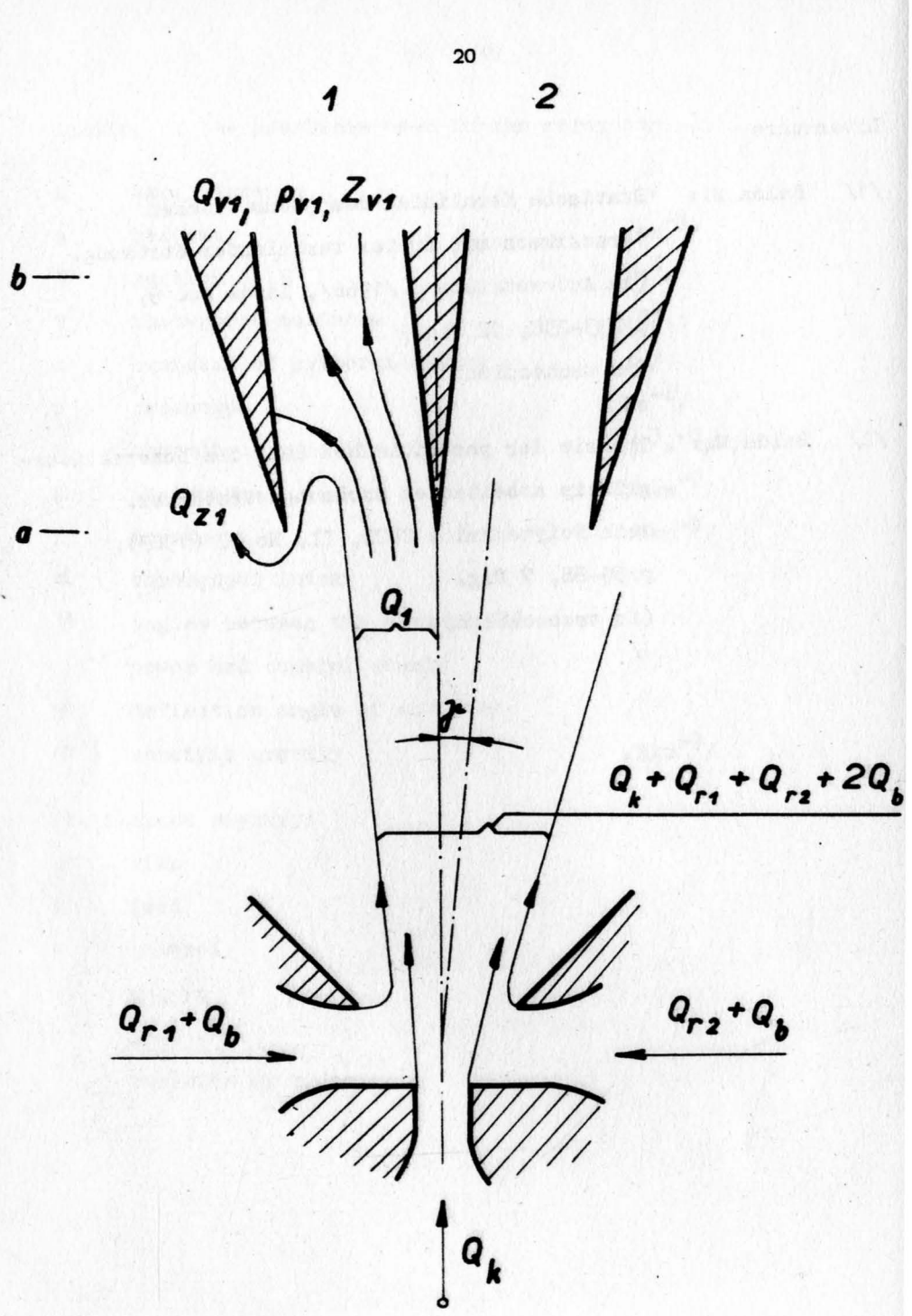

Fig. 1 Course of the flow lines in a symmetrical proportional amplifier

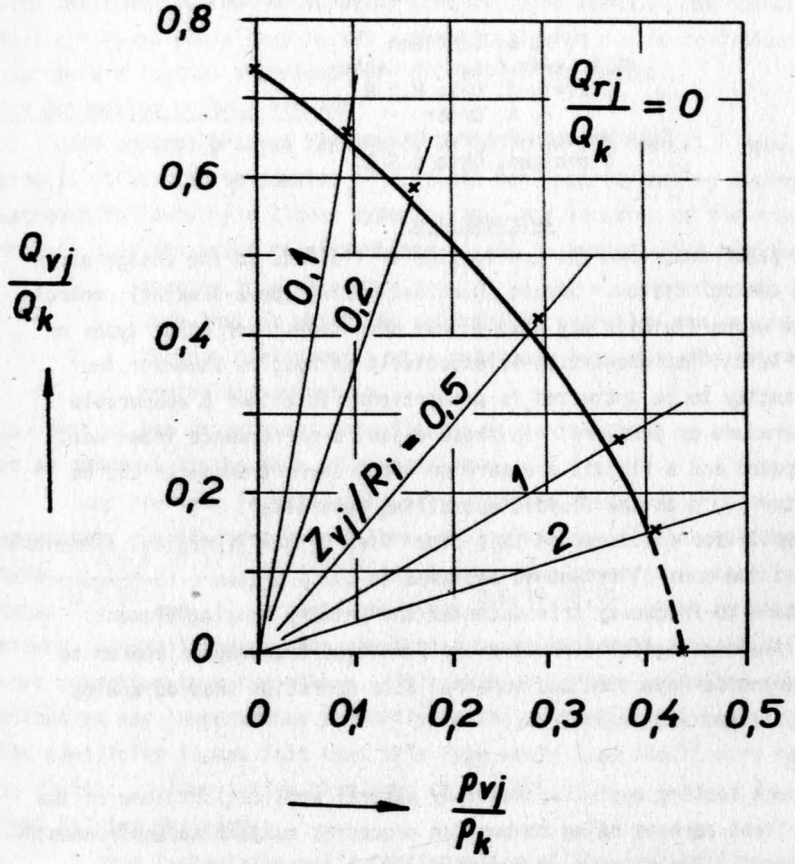

Fig. 2 Load characteristics of a CORNING's amplifier. The calculated values are marked with crosses

DEVELOPMENT OF A FLUIDIC OPTIMIZER

F. K. B. Lehtinen
NASA Lewis Research Center
Cleveland, Ohio U.S.A.
P. A. Orner
Case Western Reserve University
Cleveland, Ohio U.S.A.

Introduction

This paper describes the application of fluidics to the design of an optimizing control system. Single input optimizing (peak-seeking) control is one area where fluidics may have unique advantages over other types of control. Fluidic implementation is especially attractive whenever the process quantity to be optimized is proportional to either a measurable flow, temperature or pressure. In these cases, a performance index need not be computed and a fluidic pressure or temperature transducer can be used to interface with the fluidic optimizing controller.

The optimizer discussed in this paper uses primarily digital elements to implement the controller and is designed to use a pressure-to-frequency or temperature-to-frequency transducer as the primary sensing element. Presently, fluidic digital circuitry and f.m.-type transducers appear to offer higher noise rejection and more reliable operation than do analog fluidic amplifiers and transducers.

Application

The peak seeking optimizer has many natural applications, one of the most significant perhaps being combustion processes subject to environmental disturbances. For example, a burner could be statically optimized by maintaining stoichiometric temperature in the face of changes in ambient air density. It is feasible in this case to speak of closing the loop directly with a temperature sensitive fluidic oscillator.

An obvious advantage of the fluidic implementation is the ability to use process fluids for signal processing eliminating the need for an auxiliary power source. This could be crucial if, for instance, one wished to control a mobile (or remote) installation where electrical power was at a premium (or unavailable).

The optimizer described in this paper is being studied for application to automotive engine control. A project underway in the Systems Modelling and Control Group at Case Western Reserve University is addressed to the fluidic implementation of fuel injection for automotive engines. The optimizer would be used to close a "second level" loop around the engine by sensing the exhaust temperature, which is closely correlated

with the specific fuel consumption (and emission level). The operating fuel-air ratio would thus be set automatically for cruise conditions, with appropriate logical overrides for "off-design" operation.

The Optimizing Control Problem

The control problem considered is depicted in Figure 1. Here, the process is assumed to consist of a static nonlinearity having a single extremum followed by a linear dynamic lag. The location of the extremum depends upon the value of disturbance u. It is assumed that u either:

1. changes in a step-wise fashion but at a frequency much lower than that at which the optimizing controller can respond, or,
2. changes continuously at a rate much less than the rate of the controller output, m.

The task of the otpimizing controller is to manipulate m so as to keep p at an extremum in the face of changes in u.

Many previous investigators have attacked this same problem. Their approaches can be grouped into three main classes: (1) Peak holding types types [1,4,6,9,10,11,12,13,14,15] (2) Output sampling or incremental logic types [3,7,16] and (3) Perturbation types [2,5,17,18,19]. Peak holding optimizers, generally being the simplest type to implement, have received more attention than the others. In examining various optimizer schemes, attention was concentrated primarily on the peak holding types. Due to its simplicity it was felt that this type would lead itself more readily to fluidic implementation than some of the others.

Peak Holding Optimizers

Figure 2 shows the basic configuration of the peak holding optimizer, the distinguishing features being the relay and integrator which cause m(t) to have at a constant rate, either positively or negatively. Various schemes have been used in optimizing controller design to switch e(t) based on the delayed optimum signal p*(t) so that p(t) is driven to the optimum. Some investigators [1,4,11,13,14,15] have used peak detector circuits to detect when p*(t) has passed a peak, and thereby reversing e(t). Others [4,9,10,12] have used first or higher order derivatives of p*(t) and logic to determine when to switch e(t).

The technique chosen for use in the fluidic optimizer is one based on detecting the sign of $\frac{dp^*}{dt}$ and was developed by Broekstra, et. al. [10]

The control law for maximizing p can be stated as follows:

"Superior numbers refer to similarly-numbered references at the end of this paper."

1. If sgn $\frac{dp^*}{dt}$ changes from positive to negative, switch e(t).
2. If sgn $\frac{dp^*}{dt}$ changes from negative to positive or if sgn $\frac{dp^*}{dt}$ remains positive do not change e(t).
3. If sgn $\frac{dp^*}{dt}$ remains negative longer than a certain time T_f, switch e(t) at $t = n T_f$, $n = 1, 2, \ldots$ This is the "forced-switching" mode of operation.

Broekstra has demonstrated that this control law will cause p(t) to converge to and hunt about the extremum for a rather wide variety of process dynamics.

Digital Fluidic Optimizer

The block diagram of the digital fluidic optimizer employing Broekstra's control laws is shown in Figure 3. The process considered is composed of a parabolic nonlinearity followed by a first order lag. Process output $p^*(t)$ is converted into a pulse frequency signal, $f_p(t)$, so that computations can be performed digitally. The key to the optimizer's operation is the $\frac{\Delta p^*}{\Delta t}$ computation logic. A digital approximation to $\frac{dp^*}{dt}$ is performed as follows. As shown in Figure 4, the bidirectional counter is counted up or down by $f_p(t)$ pulses as dictated by the timing logic. The count in the counter at the end of the up counting period is proportional to the average value of $f_p(t)$ during that time (T_c). Similarly, the difference between the counter value at the end of the up count period and that at the end of the down count period is proportional to the average value of $f_p(t)$ during the down count period. The difference between these two average frequencies is then proportional to $\frac{-\Delta f_p}{\Delta t}$ and hence $\frac{\Delta p^*}{\Delta t}$. Note that this is true for a p*-to-frequency converter whose output frequency decreases with an increase in $p^*(t)$. But the content of the counter at the end of the down count interval is just the negative of this average frequency difference. Thus, to detect the sign of the average value of $\frac{dp^*}{dt}$, all that is required is logic to detect whether or not the bidirectional counter underflowed during the down count interval. If underflow occurred, sgn $\frac{\Delta p^*}{\Delta t}$ is less than zero. The actual operation of the $\frac{\Delta p^*}{\Delta t}$ computation logic will be more closely analyzed in the next section.

The sgn (e) and forced switching logic are simply a logic implementation of the scheme previously outlined.

Hunting Loss Analysis

In order to determine optimum values for sampling rate, counter size, converter frequency range and integrator gain, a hunting loss analysis was conducted for the optimizer with no process dynamics. Morosanov[4] has analyzed a similar optimizing control system using a harmonic balance method. His model includes possible hysteresis in the computation of $\frac{dp^*}{dt}$ but it doesn't consider sampling or quantization.

For the purposes of this analysis, the hunting loss is defined as

$$H = \left| \frac{p_{min} - p_o}{P} \right| \tag{1}$$

where $p_{min} - p_o$ is the peak-to-peak amplitude of the resulting limit cycle about the optimum and $-P$ is the minimum value of p. It is assumed that p_{max} is equal to zero.

The nonlinearity is assumed to be

$$p(t) = -K_m[m(t)]^2 - p_o \tag{2}$$

The integrator can be described by

$$\dot{m}(t) = A\, e(t) \tag{3}$$

where $e(t) = \pm 1$, determined by the sgn (e) logic. The p-to-frequency converter is assumed to be linear and can be described as

$$f_p(t) = f_{min} - (f_{pmax} - f_{pmin}) \frac{p(t)}{P} . \tag{4}$$

f_{pmax} and f_{pmin} are the bounds of $f_p(t)$. Assuming that $f_p(t)$ is a continuous function of time, i.e. $f_p(t)$ is much higher than the highest important frequency component of p(t), the up-down counter can be modeled as an integrator within a sampling interval. For a cycle starting at time $t = T_x$ with the counter just reset the counter value at the end of a period $2T_c$ is:

$$e'(T_x + 2T_c) = \int_{T_x}^{T_x+T_c} f_p(t)dt - \int_{T_x+T_c}^{T_x+2T_c} f_p(t)dt \tag{5}$$

If T_x occurs T_c seconds before p(t) reaches its maximum, $e'(T_x + 2T_c)$ will be zero because $f_p(t)$ integrated between T_x and T_c will be the same magnitude as $f_p(t)$ integrated between $T_x + T_c$ and $T_x + 2T_c$ (due to the symmetry of the p-m relationship). Thus, the system must continue on unswitched

for another sample period ($2T_c$).

To minimize the deviation of p from its peak value, the system should be able to detect a sign change in $\frac{dp}{dt}$ at the end of the next sampling interval. Assume that at $t = 0$, $e = +1$, $m_o = 0$, $p = -p_o$ and the down counting portion of the sampling interval has just begun. The counter value at the end of the next sampling interval, $e'(3T_c)$, can be found by substituting for $f_p(t)$ in equation (5) from equations (2), (3), and (4). The result is

$$e'(3T_c) = \frac{-4K_m A^2}{p} (f_{pmax} - f_{pmin}) T_c^3 \tag{6}$$

In order to detect that $\frac{dp}{dt}$ is less than zero, $e'(3T_c)$ must be less than or equal to minus one pulse. However, a $\pm$ 1/2 count round off error can occur during both the up and the down counting interval. In the worst case both errors will add, thus $e'(3T_c)$ must be less than or equal to -2. Substituting into equation (6), we obtain the constraint equation

$$\frac{4K_m A^2}{p} (f_{pmax} - f_{pmin}) T_c^3 \geq 2 \tag{7}$$

The hunting loss can be calculated by substituting for p_{min}, $p(3T_c)$. H is then

$$H = \frac{9K_m A^2 T_c^2}{p} \tag{8}$$

To insure that the n bit binary bidirectional counter never overflows, we write the following constraint.

$$f_{pmax} \cdot T_c \leq 2^n - 1 \tag{9}$$

The design problem is thus to minimize H as given by equation (8) with the constraints of equations (7) and (9). A simple check shows that the solution occurs for both constraints in force as equality constraints with the result that the minimum H is given by

$$H = \frac{9}{2(2^n-1)} \quad \frac{1}{1-\bar{f}_p} \quad , \tag{10}$$

where $\bar{f}_p \triangleq f_{pmin}/f_{pmax}$.

For minimum H, n is made as large as is feasible and $\bar{f}_p$ is made as small as possible. However, f_{pmin} should always be much larger than the maximum expected frequency component of p(t) in order for the assumptions leading to equation (5) to be valid. This means that f_{pmax} should equal the maximum allowable counter count rate. Equation (10) is plotted in

Figure 5 showing predicted hunting loss for typical ranges of $\bar{f}_p$ and n. Once $\bar{f}_p$ and n are selected, T_c can be found using equation (9) and the gain factor, $\frac{K_m A^2}{p}$ found using equation (7), thereby completing the design.

Fluidic Circuits

The optimizer as diagrammed in Figure 3, was implemented fluidically and is shown in Figure 6. The process nonlinearity is a proportional beam deflection amplifier using a single supply-jet and a centered receiver for the output. Process dynamics are simulated by a simple restrictor and volume combination. The integration is performed by a conventional fluidic bootstrap integrator. A pressure controlled oscillator is used as the p*-to-frequency converter and is fashioned using two NOR gates and a bistable amplifier.

The fluidic optimizer logic, which accepts $f_p(t)$ as an input and produces e(t) as an output is shown in detail in Figure 7. It is composed of four sections: timing logic, sign $\dot{p}$ logic, sign e and forced switching logic, and an eight bit binary bidirectional counter. The timing logic causes signal $f_p(t)$ to count the counter up and down, and resets the counter periodically according to the sequence shown in Figure 4. Sign $\dot{p}$ logic detects whether a counter underflow occurs during the down counting interval, and if it does, RS_2 is reset indicating $\dot{p}$ is negative, otherwise RS_2 is set. The sign e and forced switching logic causes drive signal e(t) to reverse whenever RS_2 goes from set to reset. If RS_2 remains reset long enough, PG_3 will allow forced switching oscillator O_F to trigger T_2 thereby also reversing e(t).

A worst case design approach was used in designing the optimizer logic. Static empirical models of the digital elements were used as a basis for this technique. The variation of element output impedance curves and input switch point location was determined for a batch of "typical" elements. A trial-and-error approach was then used to check whether or not all elements would be able to switch their respective load elements under worst case conditions. When necessary, supply pressures were adjusted, bleed restrictors added, or parallel elements used to insure worst case operation. This approach proved to be effective in predicting satisfactory circuit performance for frequencies up to about 250 pulses per second. Details of these circuit design methods are contained in reference 20.

Most of the logic was fabricated in semi-integrated form to minimize interconnection problems and increase logic speed, especially for the bidirectional counter. Figure 8 shows one of two four-bit counter modules used. The module was cast using aluminum filled epoxy in a silicone rubber mold. Typical supply nozzle dimensions are .015" by .025" The timing, sign and forced switching logic (Figure 9) was made using individual epoxy elements clamped in a plexiglas matrix plate, similar to a method used by Aviation Electric Ltd. Figure 10 is a photo of a bread-board version of the entire system including the optimizing controller and process.

Test Results

Transient response and hunting loss tests were made of the optimizer. The process nonlinearities used for all tests are shown in Figure 11 for u(t) = 0 and two values of R_{p1}. The pressure controlled oscillator has a characteristic as shown in Figure 12. An attempt was made to obtain the smallest possible value for $\bar{f}_p$ at the sacrifice of linearity, since the transducer need not be linear for the optimizer to function properly. f_{pmax} was made as large as the counter could handle reliably. T_c was set at 1.10 seconds, allowing a small margin of safety to prevent counter overflow.

Optimizer response curves for three different values of loop gain and no process dynamics are shown in Figure 13. As loop gain is decreased, hunting loss decreases as expected; however, response is slower. In all three cases, m(t) was set initially at an off-optimum value with the loop open at the input to the pressure controlled oscillator. Responses started when the loop was closed. For the lowest gain value shown hunting loss is approximately 2.5 percent. For smaller values of loop gain, it became more difficult for the $\frac{\Delta p^*}{\Delta t}$ computation circuit to detect the sign of $\dot{p}^*$ in the presence of noise, induced primarily from pulse jitter and variations in T_c. This indicates that to improve performance, more effort must be spent on developing stable analog-to-frequency converters as well as developing a stable low frequency oscillator.

Tests were also run for the optimizer with process dynamics, for a gain of $|\dot{m}|$ = 0.20 in. H_2O/sec. Figure 14 shows the optimizer response for a first order process time constant of 4.0 seconds. The hunting loss has increased to about ten percent. The hunting loss is determined by looking at the value of p on the p-m curve corresponding to the extreme value of m on the p*-m response curve.

Figure 15 shows the otpimizer response in the p*-m plane for a value of $|\dot{m}|$ = .040 in. H_2O/sec. Note that this increase in gain caused a further increase in the hunting loss. Figure 16 is a plot of the optimizer response displaying the "forced switching" mode. This simulates the case where the process nonlinearity shifts suddenly, placing the initial point above the desired static optimum. The forced switching oscillator period T_f was made equal to about six T_c. The gain was equal to the optimum gain for the case with no dynamics.

Conclusions

This paper has presented a new application of fluidics to automatic control systems. A breadboard version of a fluidic optimizer and simulated process have demonstrated the feasibility of an all-digital approach to optimizer design. The main problems in such digital implementations were found to be analog-to-frequency converter stability and sampling clock accuracy. A method for selecting optimizing controller design parameters has been developed. Future work will be concerned with the application of the optimizer to "real" processes, in particular, combustion temperature maximization.

Acknowledgements

This work was supported by the Fluidic Research Program of the Systems Modelling and Control Group, Engineering Design Center, Case Western Reserve University.

References

1. Draper, C.S., and Y.T. Li, "Principles of Optimalizing Control Systems and an Application to the Internal Combustion Engine," published by ASME, New York, New York, September 1951.
2. Vasu, G., "Experiments with Optimizing Controls Applied to Rapid Control of Engine Pressures with High-Amplitude Noise Signals," ASME Transactions, pp. 481-488, April 1957.
3. White, B., "The QUARIE Optimal Controller," Instruments and Automation, Vol. 29, pp. 2212-2216, November 1956.
4. Morosanov, I.S., "Methods of Extremum Control," Automation and Remote Control (English Translation) Vol. 18, No. 11, pp. 1077-1092, November 1957.
5. Schweitzer, P.H., C. Volz, and F. Deluca, "Control System to Optimize Engine Power," SAE Technical Paper 660022, January 1966.
6. Mamzic, C.L., "Potential Applications of Peak Seeking Optimizers," Moore Products Co. Technical Paper 5702, 1961.

7. Sevcik, M., "Pneumatic Digital Optimizing Device," Proceedings of the Second Cranfield Fluidics Conference, Paper No. K1, January 1967.

8. Frait, J.S., and D.P. Eckman, "Optimizing Control of Single Input Extremum Systems," JACC, ASME Paper No. 61-JAC-13, June 1961.

9. Hamza, M.H., "Extremum Control in the Presence of Variable Pure Delay," Proceedings of the Second IFAC Symposium on the Theory of Self-Adaptive Control Systems, pp. 290-298, September 1965.

10. Broekstra, G., C.J.D.M. Verhagen, and J.A. van Arkel, "A Multi-Dimensional Self-Optimizing Control System Involving Dynamics and Disturbances, Employing Relay Extremum Control," Proceedings of the Second IFAC Symposium on the Theory of Self-Adaptive Control Systems, pp. 263-273, September 1965.

11. Fujii, S., and N. Kanda, "An Optimalizing Control of Boiler Efficiency." Proceedings of the Second IFAC Congress, pp. 380-389, 1963.

12. Perret, R., and R. Rouxel, "Principle and Application of an Extremal Computer," Proceedings of the Second IFAC Congress, pp. 527-540, 1963.

13. Shull, J.R., "An Automatic Cruise Control Computer for Long Range Air Craft," IRE Transactions on Electrical Computers, PGEC-1, pp. 47-51, December 1952.

14. Genthe, W.K.,"Optimalizing Control-Design of a Fully Automatic Cruise Control System for Turbojet Aircraft," IRE WESCON Convention Record, Part 4, pp. 47-57, 1957.

15. Tsien, H.S., and S. Serdengecti, "Analysis of Peak-Holding Optimalizing Control," Journal of the Aeronautical Sciences, Vol 22, pp. 561-570, August 1955.

16. Burt, D.A., and R.I. van Nice, "Optimizing Control Systems for the Process Industries," Westinghouse Engineer, Vol. 19, No. 2, pp. 38-41, March 1959.

17. Frey, A.L., W.B. Deem, and R.J. Altpeter, "Stability and Optimal Gain in Extremum-Seeking Adaptive Control of a Gas Furnace," IFAC Proceedings, Vol. 1, Book 3, June 1966.

18. Bakke, R.M., "Transient Optimization in Optimalizing Contorl," ASME Paper No. 62-WA-275, November 1962.

19. Eykhoff, P., and O.J.M. Smith, "Optimalizing Control with Process-Dynamics Identification," IRE Transactions, JACC, September 1960.

20. Lehtinen, F.K.B., "The Development of a Fluidic Digital Optimizing Control System," Ph.D. Thesis, Case Western Reserve University Cleveland, Ohio, January 1969.

Nomenclature

- A - integrator gain
- e - optimizing controller output
- e' - bidirectional counter value
- f_p - variable frequency transducer output frequency
- f_{pmax} - maximum value of f_p
- f_{pmin} - minimum value of f_p
- H - hunting loss
- K_m - coefficient of parabolic nonlinearity
- m - process input
- m_o - optimum value of m for fixed u
- n - an integer
- p - variable to be optimized
- p^* - delayed optimum signal
- p_{min} - minimum value of p during hunting
- p_{max} - maximum value of p during hunting
- p_o - optimum value of p for u fixed
- P - minimum value of p for any u
- S - Laplace variable
- t - time
- T_c - optimizer counting interval
- T_f - forced switching oscillator period
- T_x - value of t at the beginning of a counting interval
- τ - process time constant
- u - disturbance variable

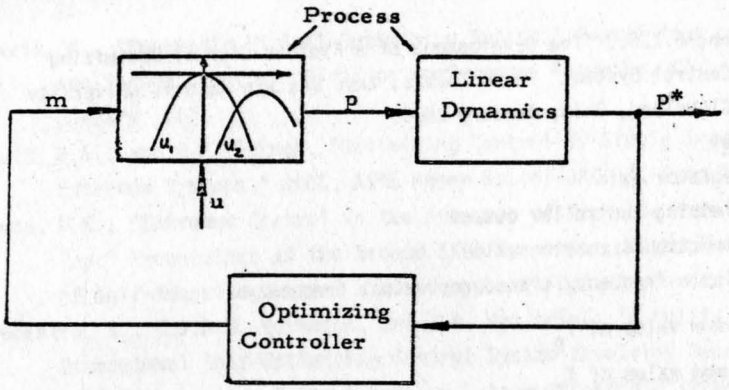

FIGURE 1 BASIC OPTIMIZING CONTROL SYSTEM

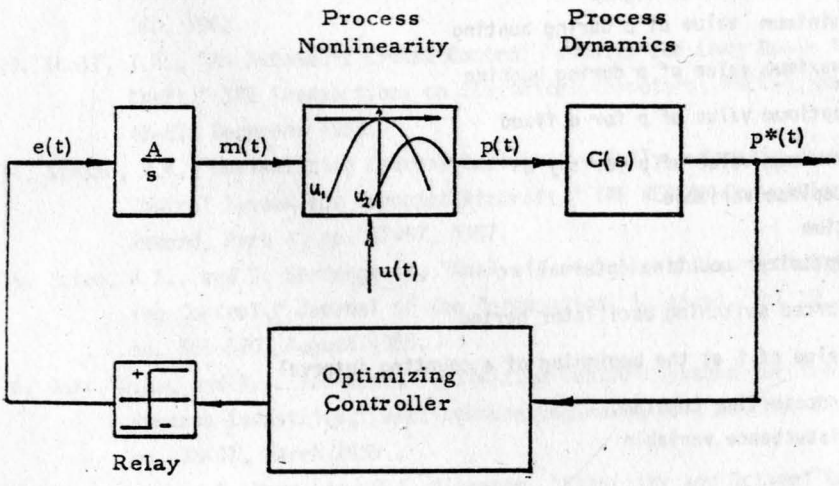

FIGURE 2 PEAK-HOLDING OPTIMIZING CONTROL SYSTEM

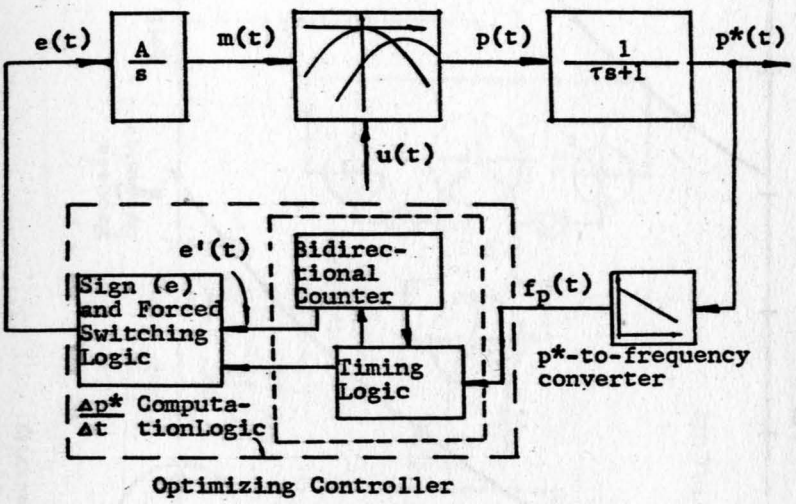

FIGURE 3 DIGITAL FLUIDIC OPTIMIZER

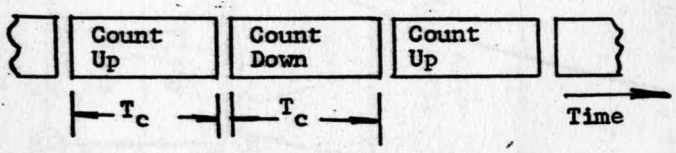

FIGURE 4 TIMING DIAGRAM FOR $\frac{\Delta p^*}{\Delta t}$ COMPUTATION LOGIC

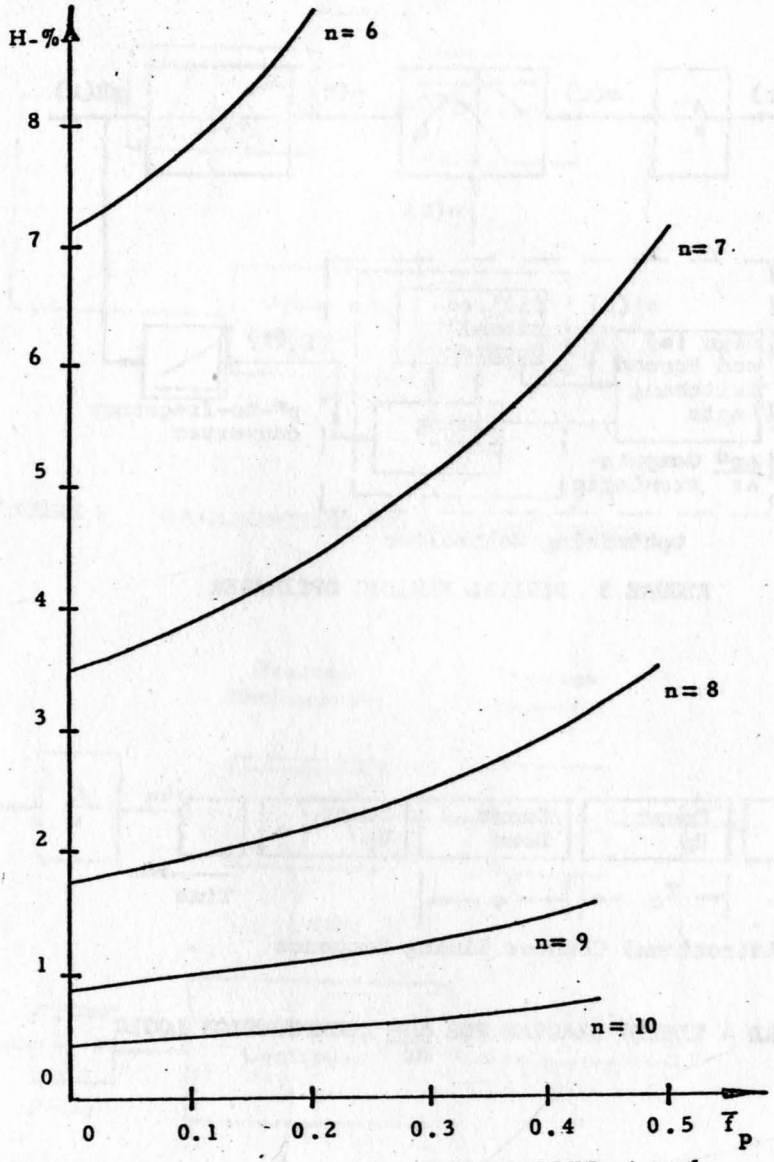

FIGURE 5 HUNTING LOSS VS. NORMALIZED p*-to-f_p CONVERTER GAIN

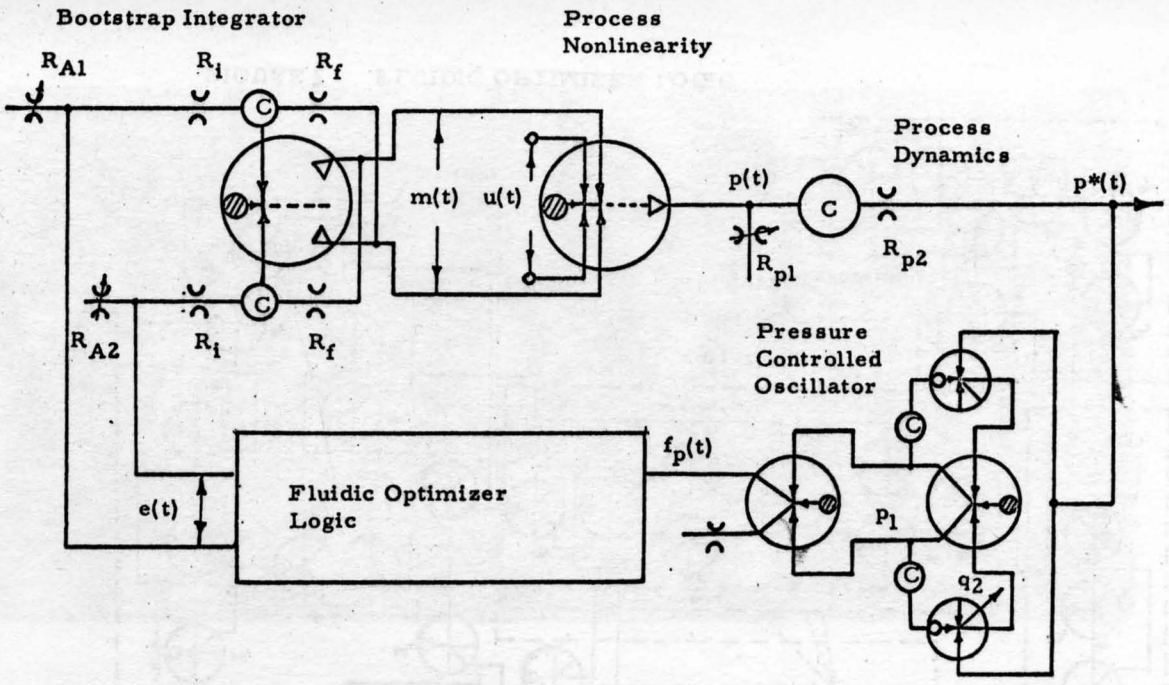

FIGURE 6 FLUIDIC OPTIMIZER CIRCUIT

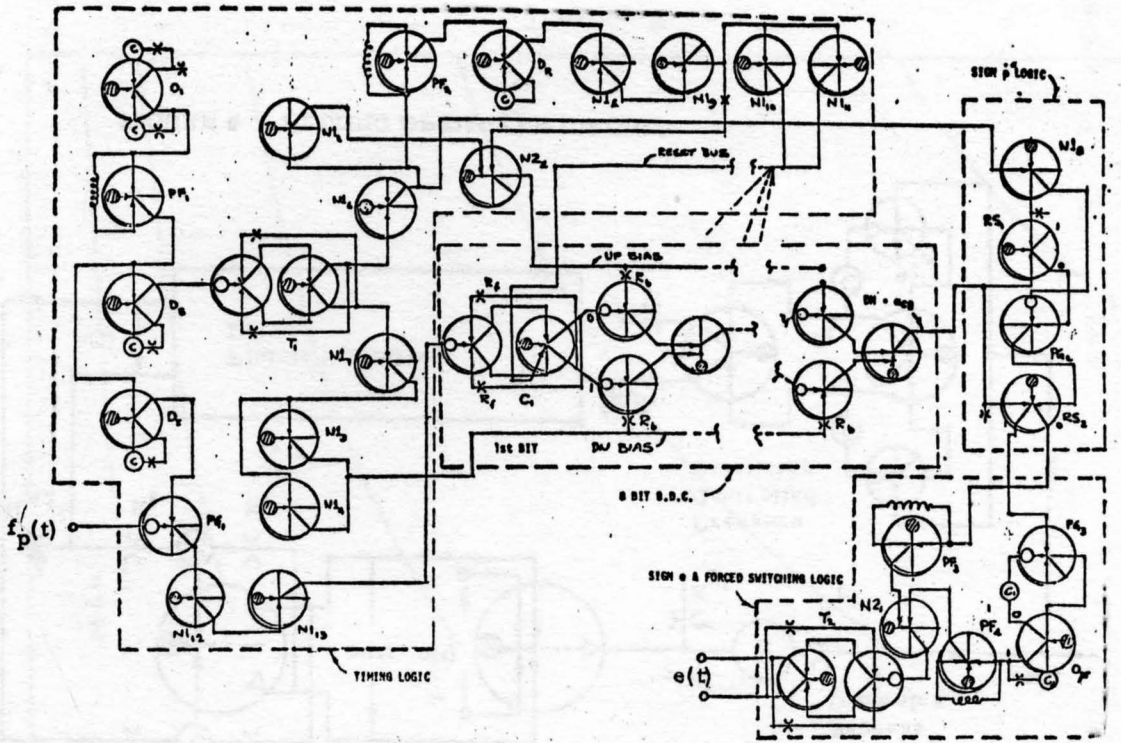

FIGURE 7 FLUIDIC OPTIMIZER LOGIC

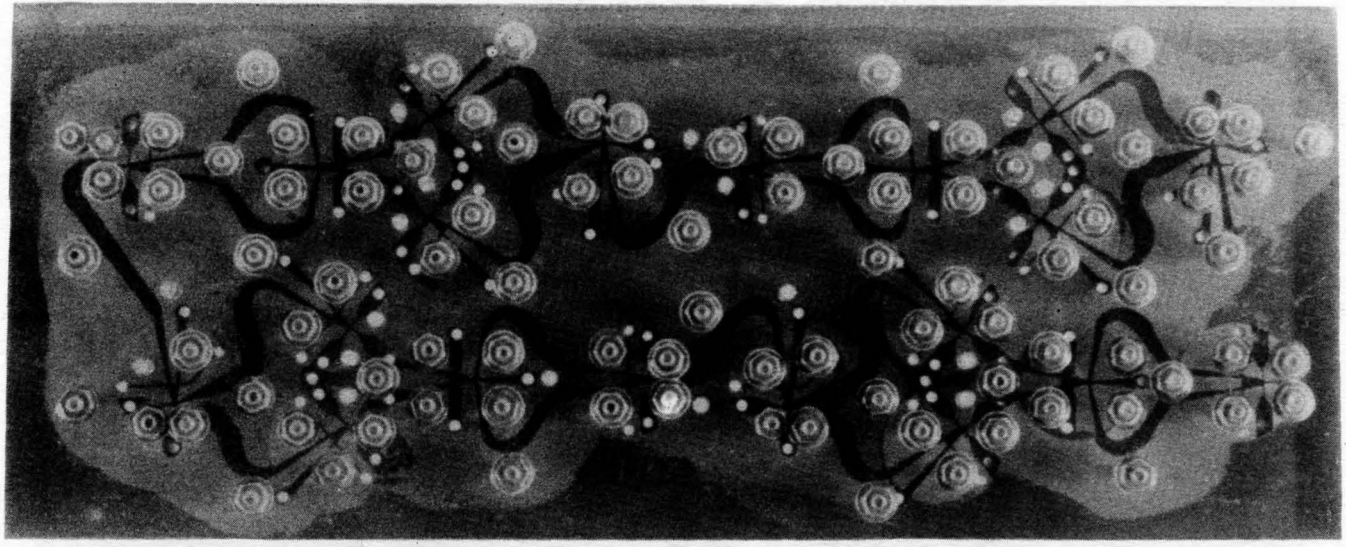

FIGURE 8 FOUR BIT BIDIRECTIONAL COUNTER MODULE

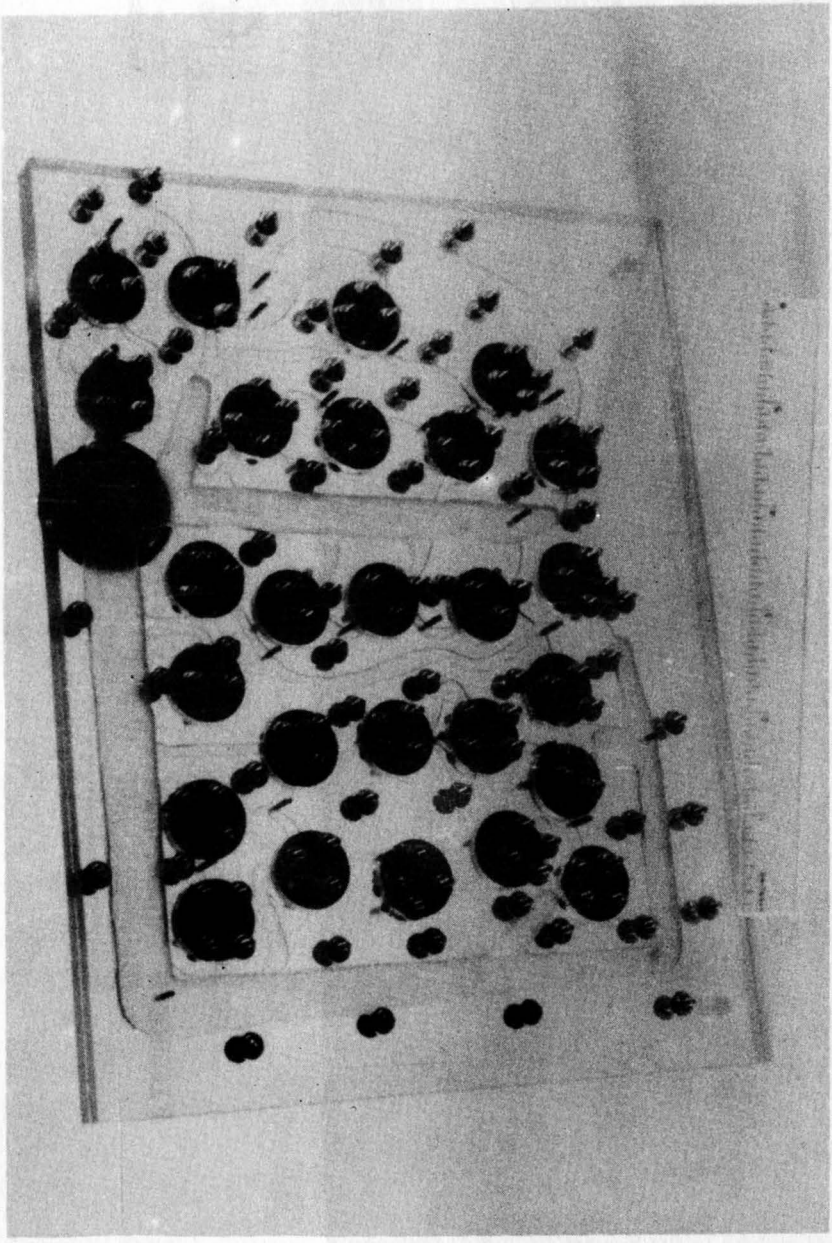

FIGURE 9 FLUIDIC OPTIMIZER LOGIC

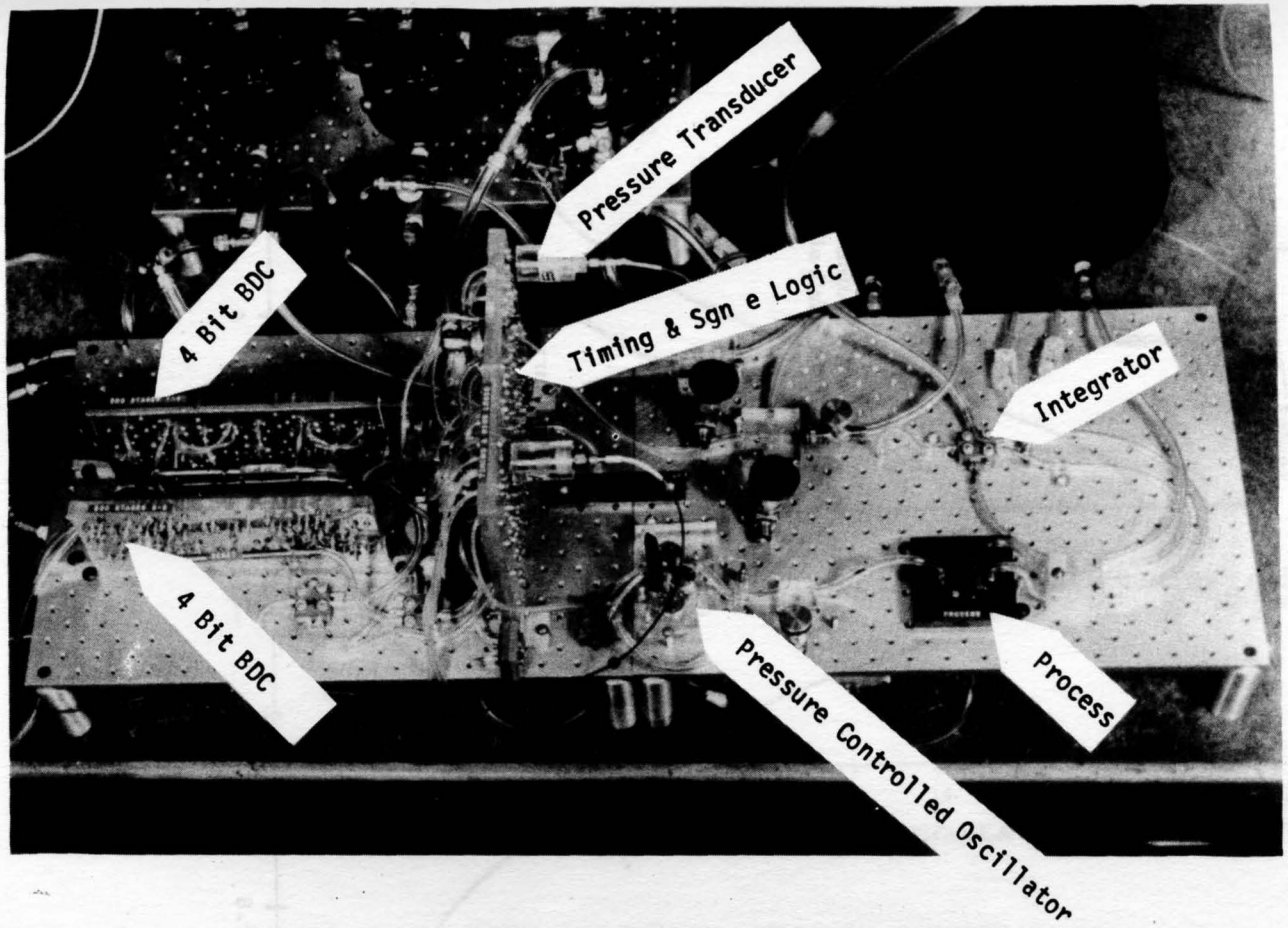

FIGURE 10 PHOTO OF DIGITAL FLUIDIC OPTIMIZER

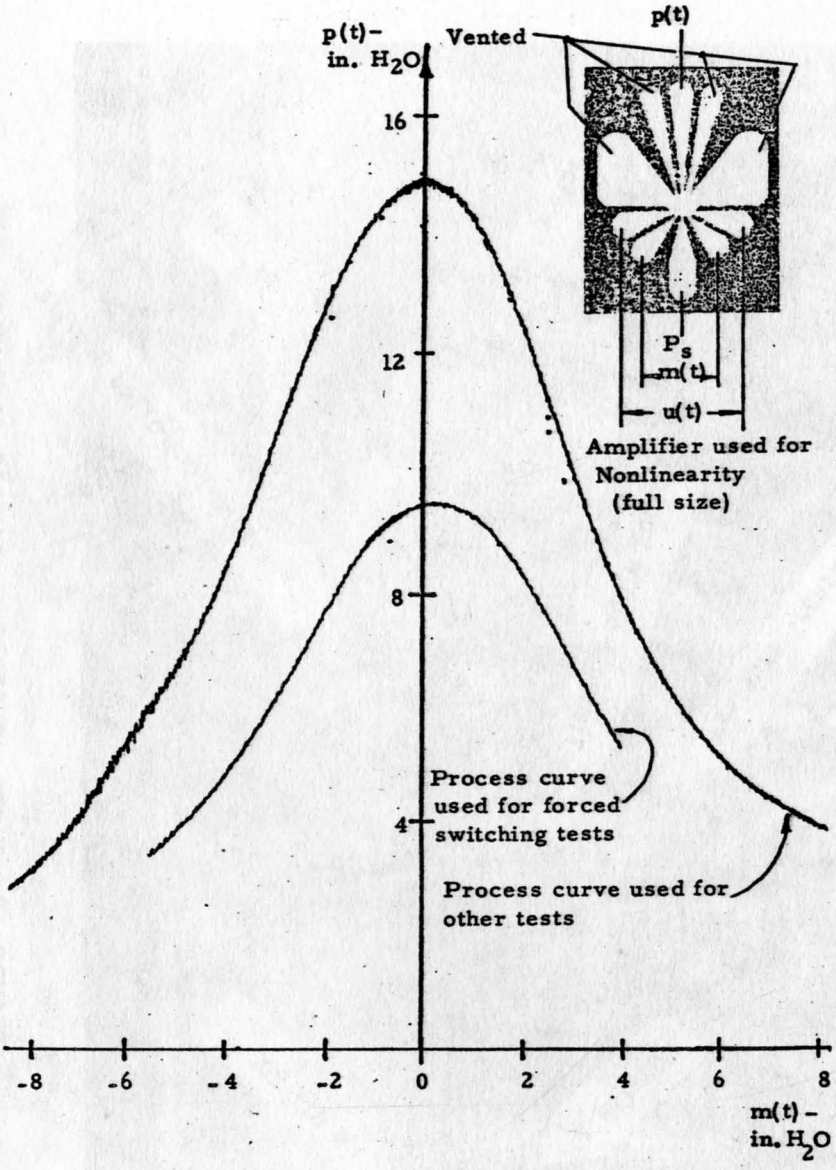

FIGURE 11. PROCESS NONLINEARITY

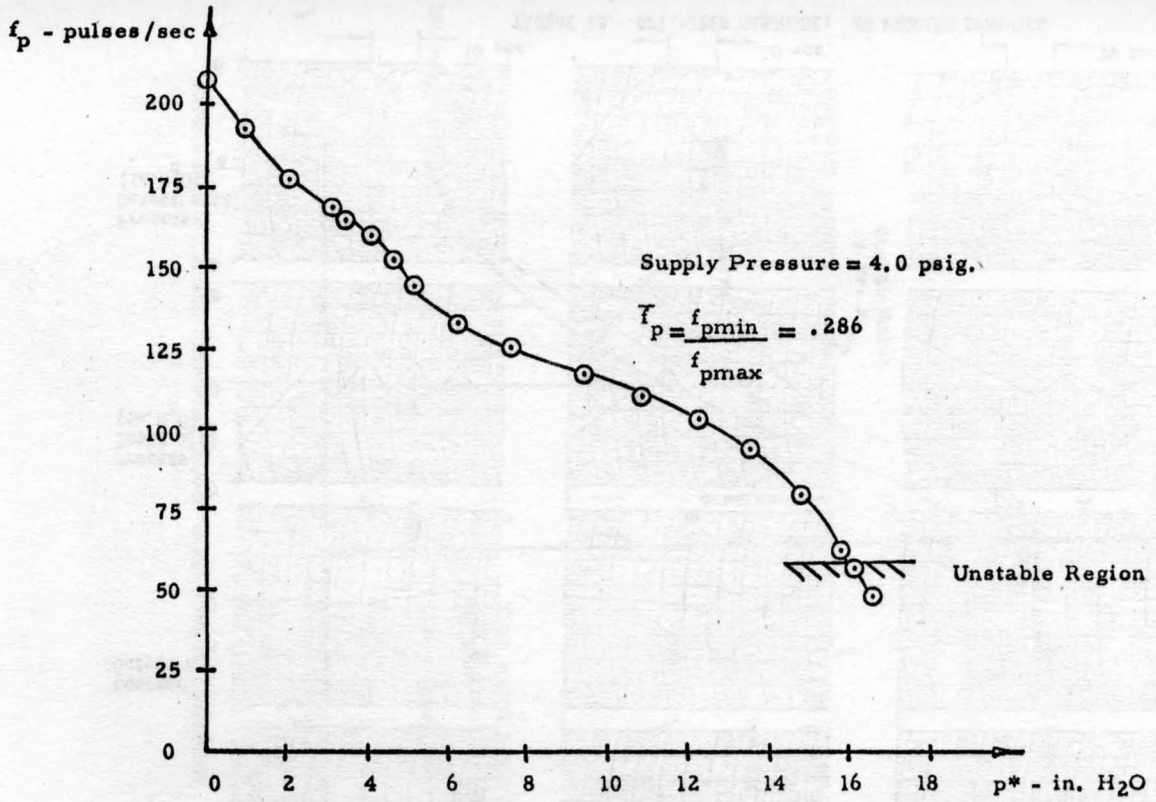

FIGURE 12 PRESSURE CONTROLLED OSCILLATOR CHARACTERISTICS

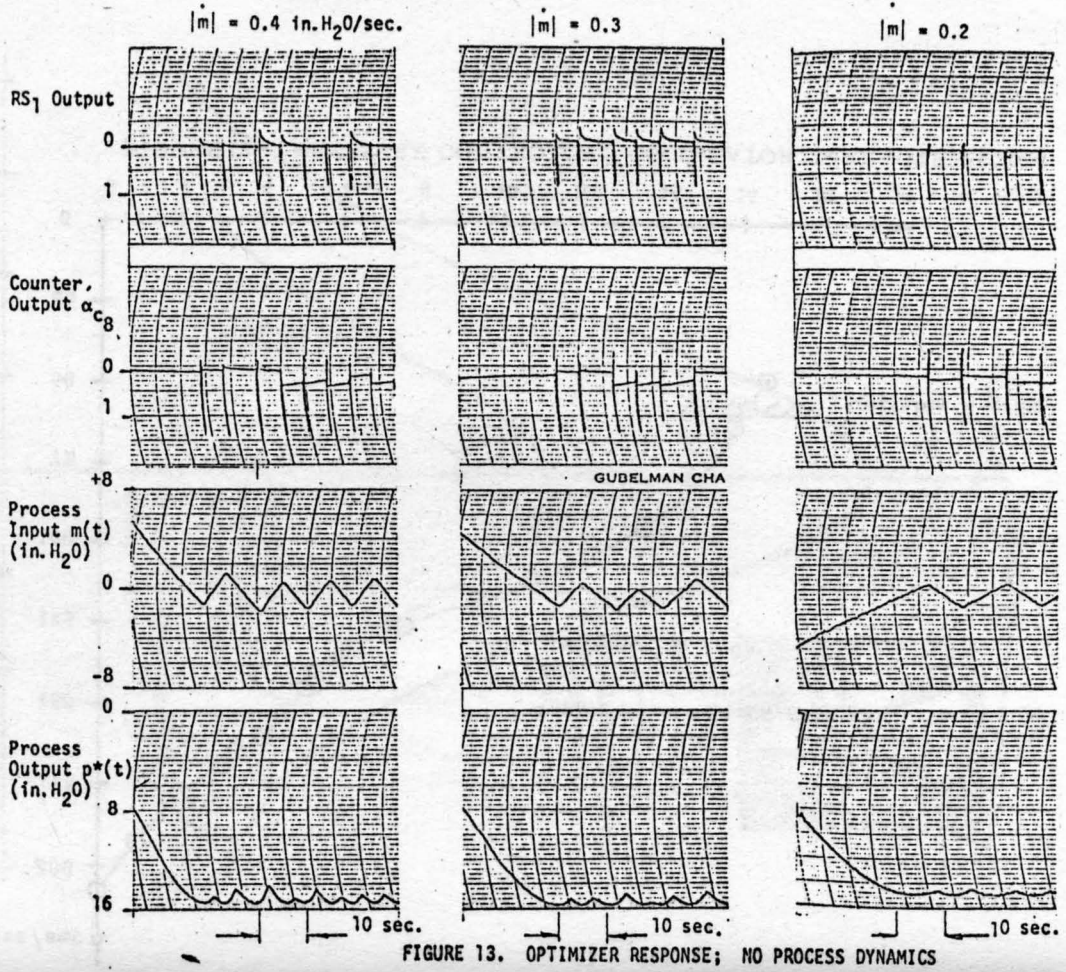

FIGURE 13. OPTIMIZER RESPONSE; NO PROCESS DYNAMICS

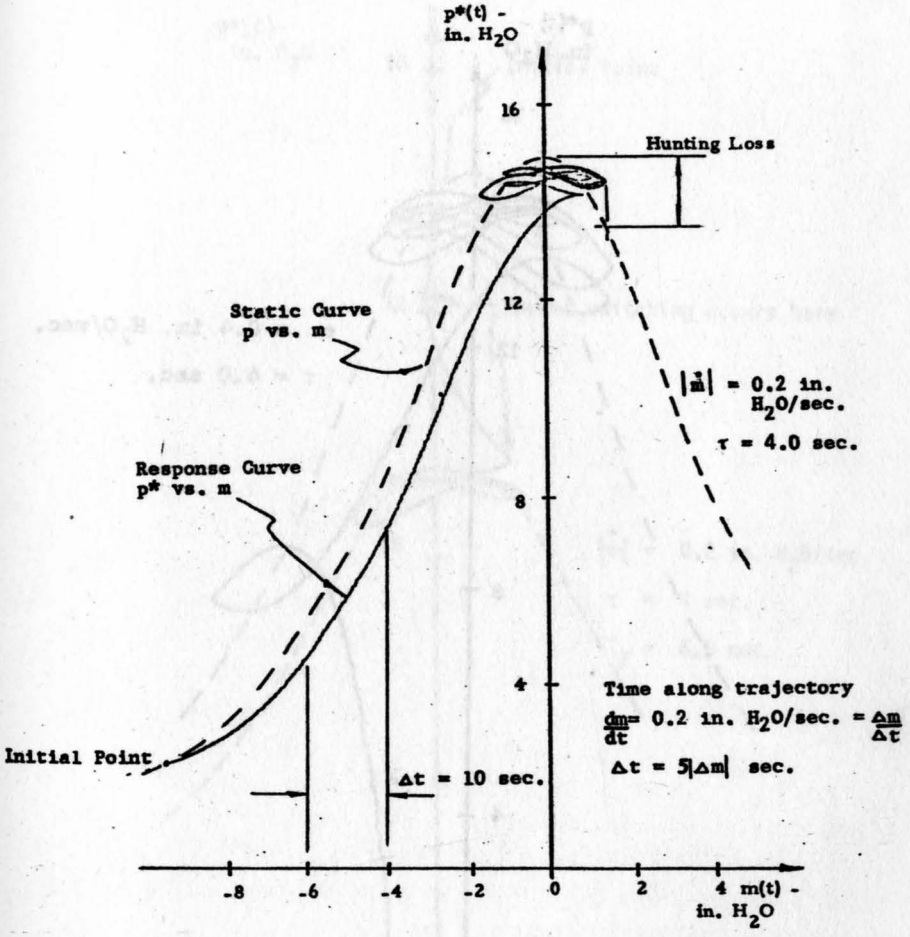

FIGURE 14. OPTIMIZER RESPONSE; FIRST ORDER PROCESS DYNAMICS

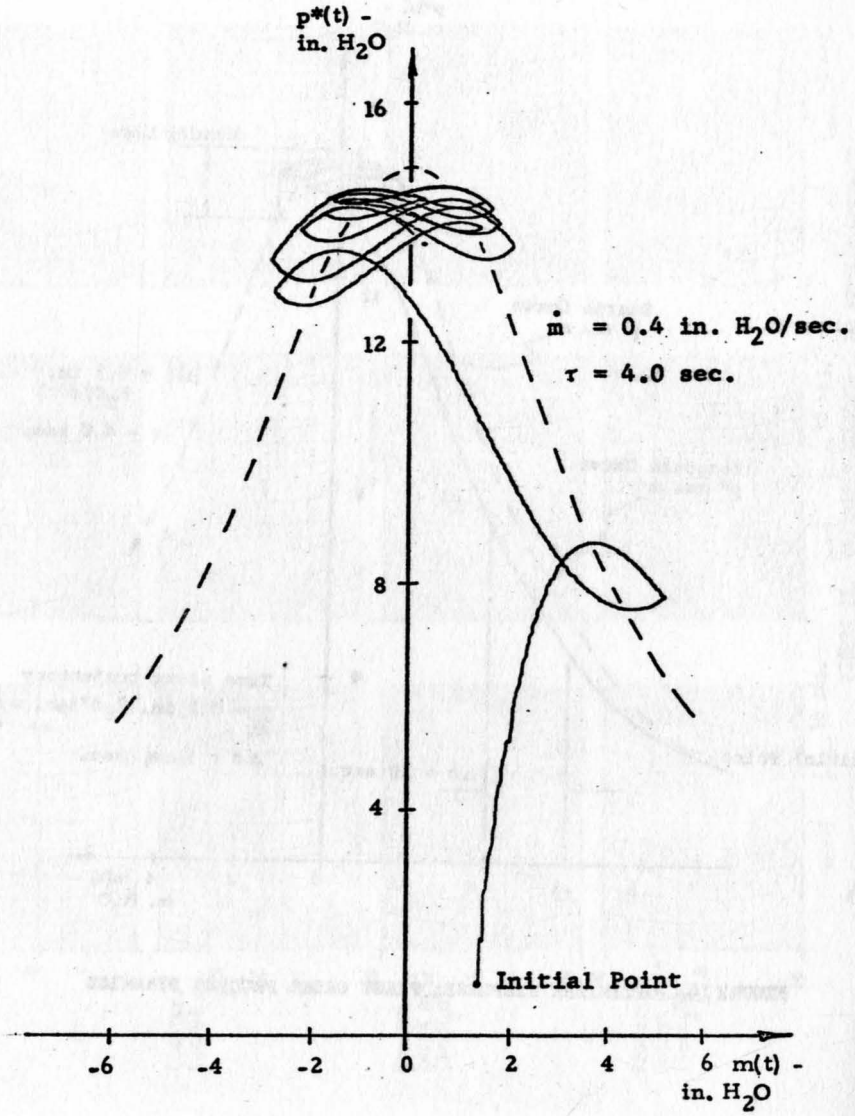

FIGURE 15 OPTIMIZER RESPONSE IN p* - m PLANE

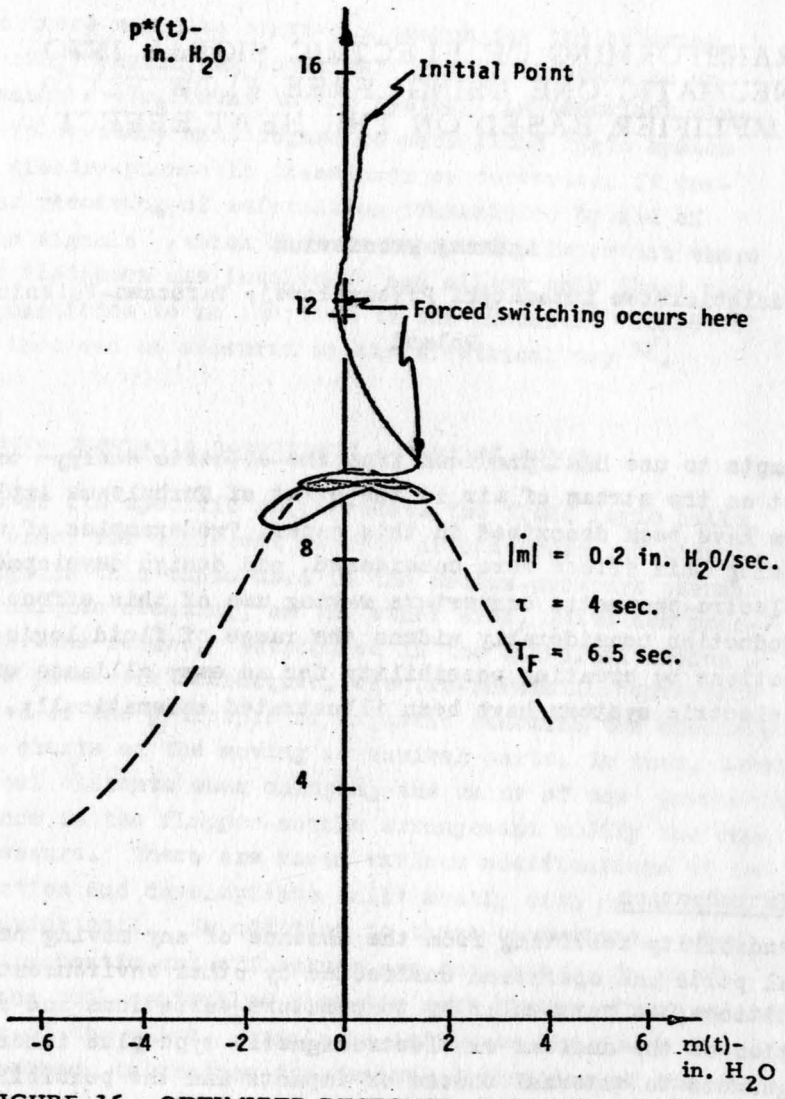

FIGURE 16 OPTIMIZER RESPONSE, INCLUDING FORCED SWITCHING

TRANSFORMING OF ELECTRIC SIGNAL INTO PNEUMATIC ONE USING FREE FLOW FLUID AMPLIFIER BASED ON THE HEAT EFFECT

Andrzej Proniewicz

Przedsiębiorstwo Automatyki Przemysłowej; Warszawa-Falenica

Poland

Attempts to use heat produced from the electric energy to react on the stream of air in the event of Turbulence Amplifiers have been described in this paper. Two examples of utilizing this effect were considered, and design developments of electro-pneumatic converters making use of this effect whose introduction considerably widens the range of fluid logic applications by creating possibility for an easy alliance with the electric systems have been illustrated schematically.

1. Introduction

Dependability resulting from the absence of any moving mechanical parts and operation unaffected by other environmental conditions, in particular by temperature variations and radiation of the nuclear or electromagnetic type plus inherent ruggedness to external shocks or impacts and the possibility for achieving considerable miniaturization have led to an intense development of the fluid logic.

Parallelly to the carried-on research work and development of logic elements constituting the central part of this technique and along with the first attempts of practical appli -

cations there was also started a search for the metering, transducing, amplifying and other type of elements as an indispensable complement to the system. An important element complementary with regard to each fluid logic system is the electro-pneumatic transducer or converter. It enables the receiving of information transmitted by aid of electric signals /which fact is especially important where greater distances are involved/ and allows only those physical quantities to be admitted to the pneumatic computer system that can be measured on the electrical way x/.

2. Electro-pneumatic converters - a brief survey

In view of its specific requirements the fluid logic calls, on one side, for different methods of conversion of electric signals than those used in the medium-pressure pneumatic techniques creating, on the other side, quite new prospects for the future. Introduced in the classical medium - pressure pneumatic techniques, electro-pneumatic converters are based on the principle of magnetic reaction the electric current exerts on the moving mechanical parts. In turn, these mechanical elements when changing the value of the pneumatic resistance in the flapper-nozzle arrangement modify the cascade pressure. There are known various modifications of the construction and developments built mostly with an incorporated moving coil. In addition to these converters, also electro-pneumatic cut-off valves are encountered in which the moving coil-controlled magnetic core blanks off or opens the seat of the valve. Trials to introduce the above described methods to produce the desired deflection of the stream do not bring the expected results since by introducing the moving elements they essentially eliminate the basic advantage offered by the fluid logic, notably its high operating reliability, and reducing the components in size is then a

---

x/ This applies to measurement of such physical quantities as for instance magnetic field intensity, radiation or determination of the chemical composition of gases.

more difficult task. When providing this brief survey of the methods for converting the electric signals into pressure signals it is noteworthy to emphasize as well the attempts made to deflect a current-conducting stream, as for instance the stream of mercury or molten metal with electric current flowing therethrough, by acting on this fluid conductor with an electromagnetic field.
Though possible to be employed also in the fluid logic, the electromagnetic dislodging of the ionized stream of gas seems to be of little practical value because of the arising necessity to introduce additional ionization equipment along with high control potentials.

Apart from the converter devices built on the principle of electromagnetic action exerted by the electric current it is also possible to take advantage of the thermal action of the electric current. Two pronciples may be distinguished in this specific case: the first based on the heating of mechanical parts which when changing in their dimensions disturb the flow, or another one based on the heating of the stream itself /direct action/.

3. Direct thermal action of the electric current exerted on the flowing stream of air

3.1. Heating of air stream

Considerations as set forth in this Chapter and relating to the pneumatic elements can essentially be widened to a great extent also to fluid elements where the liquid is used in the capacity of the working medium. The effect exerted by the heating process on the value of output pressure may be observed with regard to both Turbulence Amplifiers[5/,6/], as well as Coanda or Wall Attachment Devices [1/,2/,3/,4/]. Considerations continued hereinafter are restricted to the Turbulence Amplifiérs only and they cover the two most simple cases:

- the input of heat to the laminar flow stream at its free flowing part, and the utilization of the effect of changing specific gravity of the flowing air, and this of the growing flow losses due to higher stream viscosities.

- the input of heat applied to the stream near the point of transition from the laminar to turbulent flow at its part restricted by the input nozzle of a constant cross section, and the utilization of the effect the changing viscosity of the flowing air exerts on the character of the flow of stream.

The interaction of the electric current, through heat effect, on the laminar flow of the stream is in reality a much more complex problem and consists in the mutual interference of the changing specific gravity, viscosity and other thermodynamical phenomena.

Fig. 1. shows the layout of a Turbulence Amplifier /with no control jet/. The supply air is fed at a pressure p_z to the port 1 from where it flows out creating a stream 2/with parameters suitably selected the loss in pressure may be not very high/.

Fig. 2 /curve $t = 22^{\circ}C$/ shows the supply characteristic $p_a = f/p_z/$ of such a Turbulence Amplifier measured under ambient temperature conditions. If we put now the device tested over to the surroundings of an other temperature it will be seen that the supply characteristics plotted for the individual varying temperatures will greatly differ from each other. Fig.2 shows the family of supply characteristics plotted for various ambient temperature values. During further continued tests, the air was heated by feeding electric energy to the resistance element.

For schematical presentation of this experiment refer to Fig. 3. Fig. 4 shows the family of the supply characteristics plotted for a range of constant electric current values fed to the heater element.

Ratings of the electric current needed to transform the temperature of the stream can be found by comparing the supplied energy with the produced heat transferred upon the stream:

$$kN = C_p \cdot Sv \cdot \Delta T \qquad /1/$$

where: C_p - specific heat of air at constant pressure related to the unit of volume;

k - efficiency of the electric energy-to-stream heat conversion /1 - k dissipation of thermal energy/

N - wattage of the electric current supply;

S - stream cross-section;

v - mean rate of stream flow;

ΔT - mean increment of stream temperature.

In our simplified type of calculations, we shall not consider k and C_p as a function of the varying temperature. Assuming furthermore that the working overpressure values do not differ much from the atmospheric pressure, phenomena tested may be considered to take place at a constant pressure.

Now, diregarding air density variations and the outflow losses we can deduce the rate of stream flow from the following relationship:

$$v = \sqrt{\frac{2p_z}{\varrho}} \qquad /2/$$

where: v - mean velocity of stream outflow;

p_z - supply pressure, overpressure;

ϱ - specific mass of air;

By putting /2/ under /1/ we arrive finally at:

$$N = \frac{\pi}{2\sqrt{2}} \frac{C_p}{\sqrt{\varrho}} \frac{1}{k} d^2 \sqrt{p} \, \Delta T \qquad /3/$$

From the relationship /3/ it results for instance that in order to heat up the stream of air outflowing from an 0.4mm dia nozzle,and supplied to this nozzle at a pressure of: 500 N/sq.m, to a temperature of 100°C, we must feed in a continuous manner the supply of electric energy corresponding in terms of power to an approx. 0.2 W electric current with the heat efficiency assumed to be 100% /k = 1/.

3.2. Conversion of analogue electric signal-to-pneumafic pressure signal type

The initial part of the supply characteristic /highly

reproducible range of laminar flows/ shows a step-down tendency as the value of wattage rises. It promises the possibility of building a current converter of a continuous operation type.
If the supply parameters are now selected so as to remain stable, e.g. in a sequence of 750; 500; 380 N/sq.m /below the critical value of the Reynold's number/ and the value of current fed to the heater coil is suitably changed then we shall be able to obtain the control characteristics. Such characteristics plotted by way of experiment are shown in Fig. 5.

An element of the following parameters was subjected to testing:

Inlet nozzle diameter	d = 0.3 mm
Distance between nozzles	l = 5 mm
Pressure supplied in the order of sequence: N/sq.m	p_z= 750; 500; 380
Kanthal coil of a pressure:	R = 14 Ohms

In order to be able to compare better the individual results of the test, the following reduced function was built up:

$$\frac{Pa}{Pa_{i=o}} = f/i/$$

Diagrammatically, this function is shown in Fig. 6.
The following mathematical equation gives in some way its Approximation:

$$\frac{Pa}{Pa_{i=o}} = \frac{1}{1+ci^2} \qquad /4/$$

where:

$$c = n\frac{R}{d^2\sqrt{p}} \qquad /5/$$

The relationship as shown in /4/ provides a simplified statical characteristic of the converter shown diagrammatically in Fig. 3, and it says that the effect of current variations with regard to the output pressure will be the more clearer the greater is the numerical value of the coefficient c. the coefficient c depends in its turn on the resistance

of the electric element R, and on the second power of the supply port diameter d and square root of the supply pressure p; it is moreover dependent on the properties of the working medium and on the efficiency of heat transmission.

3.3. Descrete conversion of electric signals to pneumatic pressure signals

Another part of the supply characteristic covers the range of turbulent flows, and shows a tendency to step up along with the rise of temperature. This is chiefly so because of the ordering process taking place in the turbulent stream and proceeding parallelly with the growing viscosity of air.

When the supply pressures are selected so as to remain constant, e.g. in the following order of values: 4500; 5000;, 6000 N/sq.m /the values corresponding to turbulent flows at normal ambient temperature/, and the output pressure is measured while the electric current is fed to the heater coil then the outcome of this procedure will give as a result the control characteristics. Such characteristic curves are shown in Fig. 7, and they are typical for the relay type equipment.

As long as no electric energy supply is fed to the converter, the flowing stream will have a turbulent character

On account of a remarkable spacing between supply 1 and the output 4 there comes to an intense mixing of the unordered turbulent stream with the environmental atmosphere and high flow losses associated therewith are suffered. Accordingly, the output pressure P_a takes on a value which is much lower than the supply pressure P_z.

If now the voltage source is connected to the electro-thermal element 3, then similarly to the previous process, the

---

x/ The turbulent character of the stream flow for the nozzle of a predetermined bore may be obtained with much lower values of the supply pressure that this would result from Re_{kr} by suitably shaping the form of the supply chamber.

electric energy converted into heat will be transferred upon the stream whose temperature will rise respectively. This change of temperature will be followed by a number of other modifications in the stream parameters including those of viscosity. The increase in the stream temperature will cause a rise in air viscosity and conformity of the stream whose losses will in this connection be lower.

With the very instant the predetermined temperature limit is exceeded, the turbulent stream changes to a laminar flow stream and the output pressure accepts the maximum value $P_{a\ max}$. A further increase in the temperature will render that the process starts to take on a typical character as in the event of laminar flows and the output pressure will begin to drop somewhat.

Fig. 8 shows a modification of the subject device. In this specific case, the thermal energy is supplied through an inlet nozzle of a constant cross-section. The parameters of the stream will be chosen so as to keep the stream turbulent at the normal ambient temperature. As for the practical embodiment of this device, the change-over /switching/ stage should be preceded by a preliminary stage at which the current does not react on the character of the flow and the value of pressure is kept constant at the output until the converter is changed over.

Fig. 9 shows the reduced static characteristic of the a/m converter, obtained by experimentation.

Fig. 10 shows responses measured during the preliminary tests, relating to unitary steps and preset by switching on or off the supply of electric current.

4. Conclusion

Converters built according to the above described principle of direct thermal interaction of the electric current on the stream stand out for simplicity of design, small overall dimensions and high durability features. Their dynamic properties may be suitably adjusted by changing structural parameters as required. With average parameters in view the transmitted frequency is approximately 5 c/s. The level of the electric control signal, as it results from relation-

ship /3/, depends to a great extent on the structural parameters of the Converter. This is why, in some devices with larger transverse dimensions of the supply channel and with higher supply pressure values there arises a necessity for building a two-stage converter in which a miniature electro-pneumatic converter controls the operation of the Jet Amplifier.

This is especially important where a very low power control signal, as for instance the electric signal received from a miniature transistorized system is available;

The arrangement, called analogue, features a high reproducibility of results. The discrete converter, on the other hand, exhibits a much lower demand for electric power to actuate the control signal.

5. Figures

Fig.1: Flow of the main stream in a Turbulence Amplifier;

2: Supply characteristics of the Turbulence Amplifier measured at various environmental temperature values;

3: Layout of the analogue electro-pneumatic converter;

4: Supply characteristics of the device shown in Fig.3 measured at constant electric current values flowing through the heater coil;

5: Control characteristics for the laminar flow range;

6: Reduced control characteristics;

7: Control characteristics relating to turbulent flows;

8: Layout of a discrete converter;

9: Reduced characteristics of the discrete converter;

10: Response to unitary step preset by switching on or off the electric current supply.

6. References

1. DM. Mc. Glaughin - Electrofluidal Signal Converter; TBM - Disclosure - 1965;

2. F.D. Yeaple - Heat and Electricity Joint Air to Control Fluid Amplifiers; Product Engineering - 1967;

3. DM. Mc. Glaughin - CK. Taft - Fluidic Electrofluid Converter; Journal of Basic Engineering ASME - 1967;

4. J.Matuszewski - Fluidic Electro-Pneumatic Converter Optimization, Report EDC 7-67-16 Case Institute of Technology, Cleveland 1967;

5. P. Kupec - Elektro-pneumatischer Wandler ohne bewegte Teile - Seminarium on Microminiaturization, IFAC 1967

6. A. Proniewicz - Elektro-pneumatischer Wandler fuer Fluid-Elemente - Archiv fuer technisches Messen und Industrielle Messtechnik - 1968.

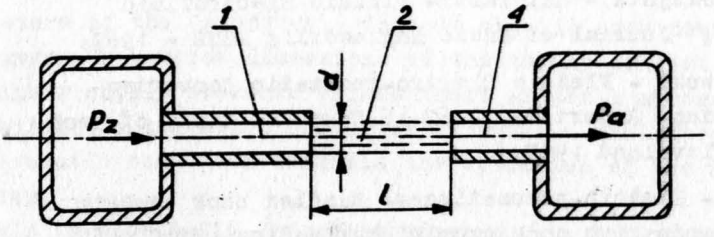
1
2
4
d
p_z
p_a
l

Fig. 1

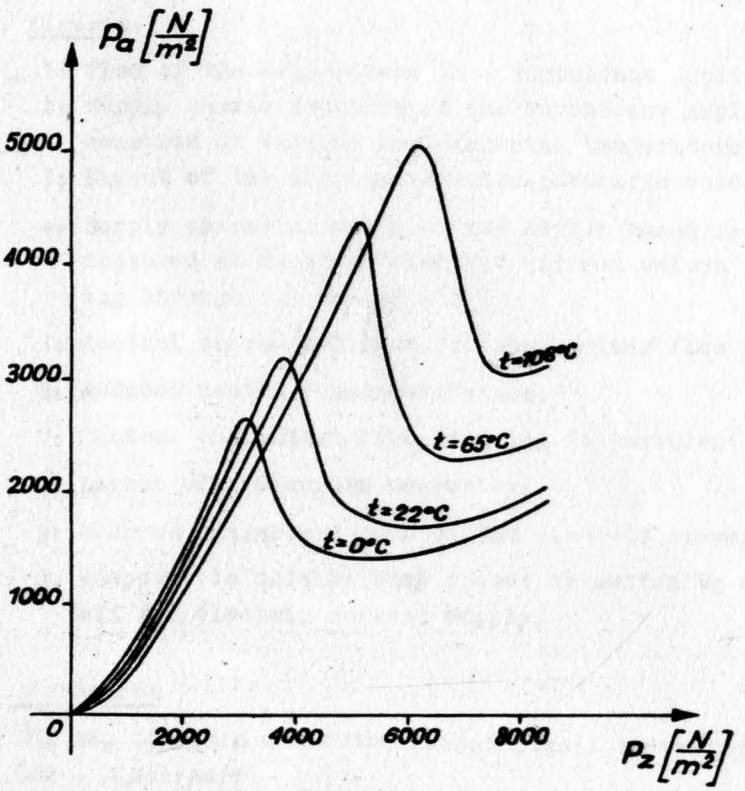
$p_a \left[\frac{N}{m^2}\right]$
5000
4000
3000
2000
1000
0
2000
4000
6000
8000
$p_z \left[\frac{N}{m^2}\right]$
t=106°C
t=65°C
t=22°C
t=0°C

Fig.2

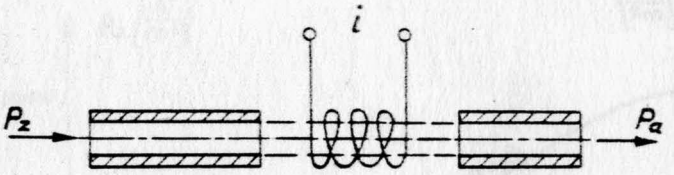
i
P_z
P_a

Fig. 3

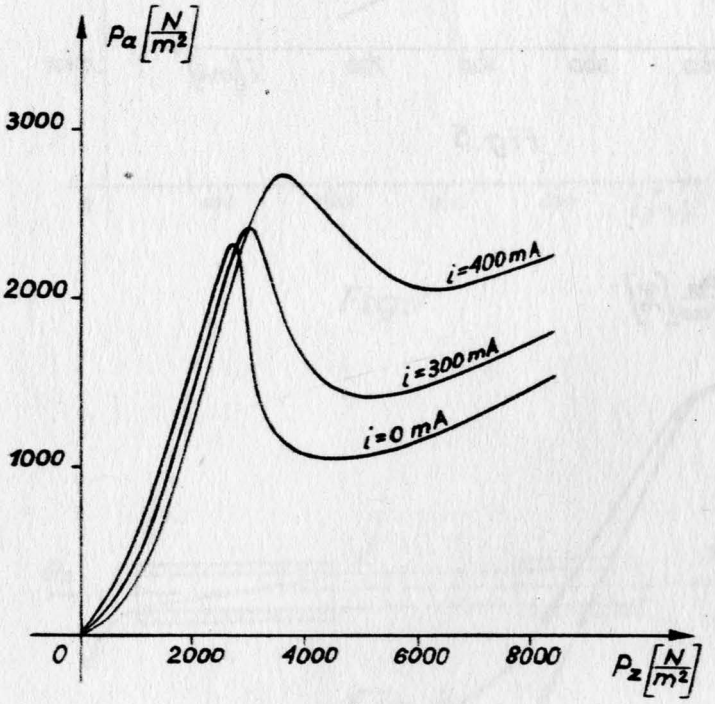
$P_a \left[\frac{N}{m^2}\right]$
3000
2000
1000
0
2000
4000
6000
8000
$P_z \left[\frac{N}{m^2}\right]$
i=400 mA
i=300 mA
i=0 mA

Fig. 4

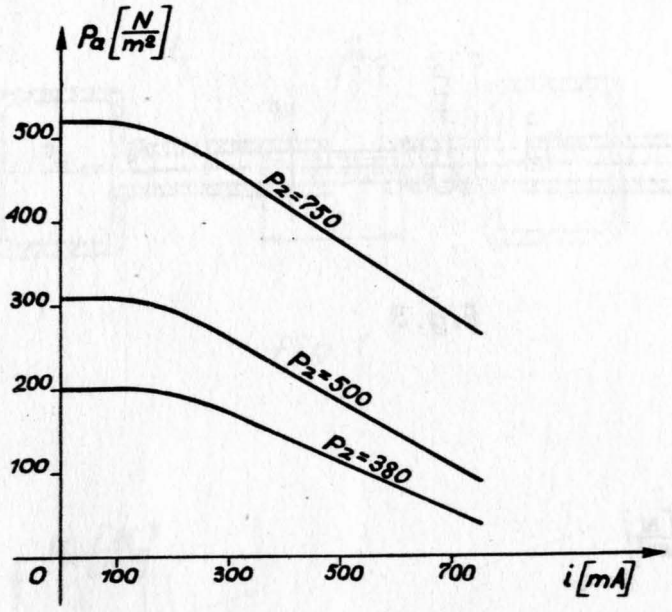
Pa [N/m²]
500
400
300
200
100
0
100
300
500
700
i [mA]
P2=750
P2=500
P2=380

Fig.5

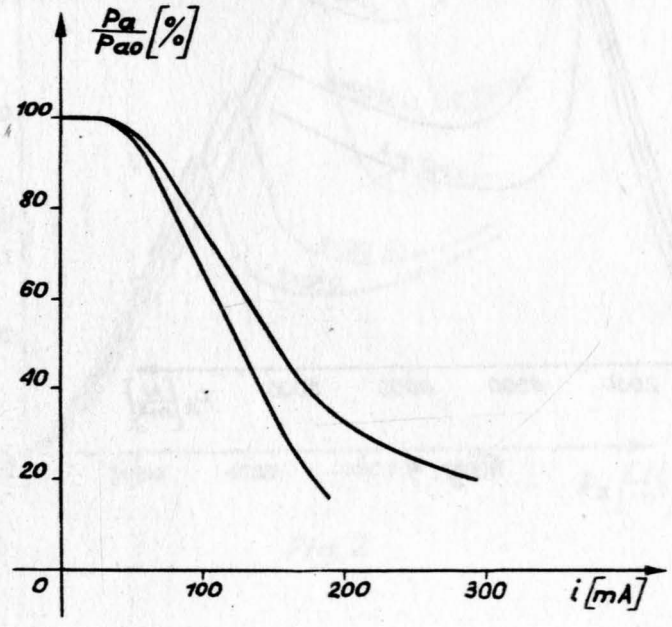
Pa/Pao [%]
100
80
60
40
20
0
100
200
300
i [mA]

Fig.6

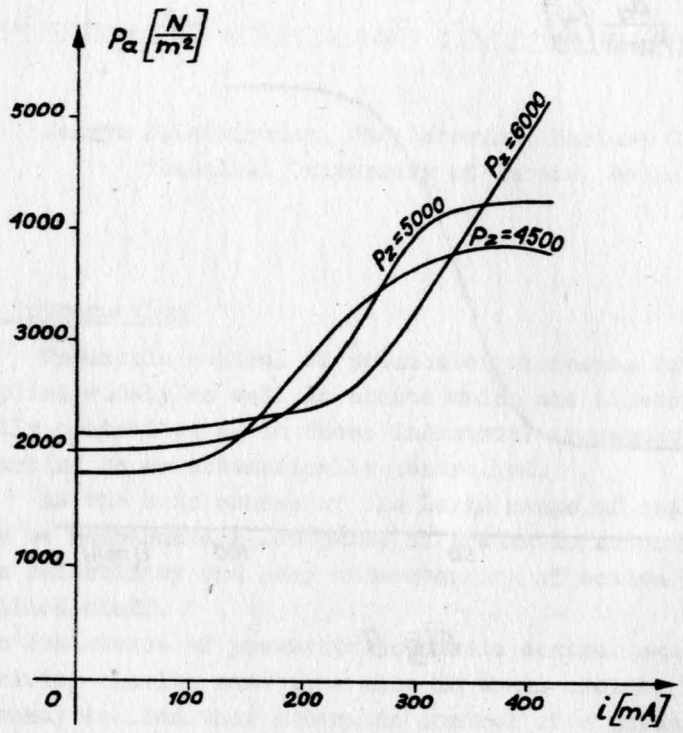
Pa [N/m²]
5000
4000
3000
2000
1000
0
100
200
300
400
i [mA]
Pz=6000
Pz=5000
Pz=4500

Fig.7

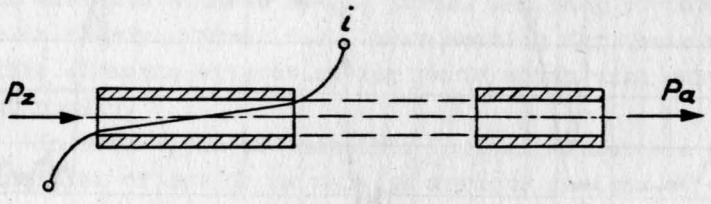
i
Pz
Pa

Fig.8

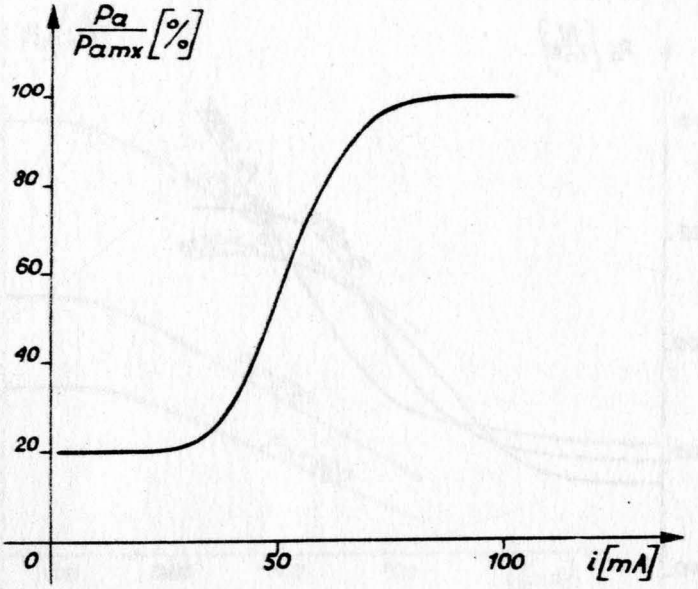
Pa / Pamx [%]
100
80
60
40
20
0
50
100
i [mA]

Fig. 9

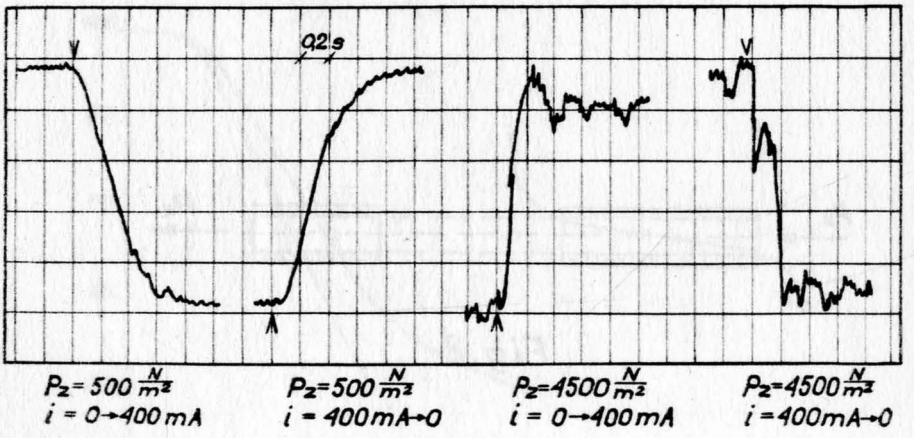
0,2 s
P2 = 500 N/m²
i = 0→400 mA
P2 = 500 N/m²
i = 400 mA→0
P2 = 4500 N/m²
i = 0→400 mA
P2 = 4500 N/m²
i = 400 mA→0

Fig. 10

PNEUMATIC MEMBRANE LOGICAL ELEMENTS

Henryk J.Leśkiewicz, Jan Jacewicz, Mariusz Olszewski
Technical University of Warsaw, Poland

1. Introduction

Pneumatic control of production processes is nowadays applied widely as well in plants which are already automatically controlled as in those industrial processes which are starting to be automatically controlled.

As the main causes of the large range of applications may be mentionned a low price of pneumatic automatic control, its reliability and easy understanding of action by a low-skilled staff.

The resistance of pneumatic automatic control against radioactivity results sometimes also in their choice. When it was already decided that automatic control of a given process has to be pneumatic, and the process is of the kind which may be controlled by logical elements, there are two main kinds of those elements to be chosen, and namely, elements with moving parts, such as spool or membrane elements, or elements without moving parts, then pure fluidics.

Elements with moving parts work with higher air pressure than elements without moving parts, and they do not use supply air in steady states, i.e., when waiting for their action, unlike elements without moving parts which take supply air continually.

In both types of pneumatic logical elements a number of principles of action as well as various designs were developed. For automatic control of a given industrial process besides a logical block consisting of logical elements, a great number of sensors, transducers, transformers, amplifiers, signal generators, punch-tape readers, and other auxilliary equipment are used. The equipment is included in a system of elements for pneumatic control together with

logical elements. The choice of logical elements affects usually the design of almost all elements of a system in this way that the accepted principle of action and individual design parts of those logical elements are used in other auxilliary elements of a system whereever possible. This increases the importance of choice of a principle of action and of a design of logical elements, thus they constitute a basis of the whole pneumatic automatic control system.

The new pneumatic logical elements are presented below, and an attempt is made to justify the choice of, as well, a principle of action, as of design.

2. The choice of a kind of elements

Pneumatic logical elements are mass products. This fact is quite essential for research on pneumatic logical elements. Thus the designed logical elements should be suitable for mass production, both for designing features and chosen materials, and on the other hand, they should find easily a wide application.

The following factors were taken into consideration:

1. membrane elements do not require so high air quality as pure fluidics, which results in better reliability of membrane elements in spite of their moving parts,
2. membrane elements have about a hundred times higher signal value than pure fluidics, which allows to avoid some pressure amplifiers in a system,
3. membrane elements may not use supply air in steady states, whereas pure fluidics, independently of their state, use continually supply air,
4. due to the lack of suitable production technology the expected lower price of pure fluidics elements than that of membrane elements has not been reached yet,
5. generally larger dimensions of membrans elements compared to those of pure fluidics are not of a great importance in stationary applications in which pneumatic logical elements are applied mostly.

From this reasons, and due to some additional considerations pneumatic membrane logical elements were chosen.

3. The principle of free membrane

In traditional pneumatic elements of automatic control, as well as discreet as analoque, the used flat membranes had always disks stiffening the central part of a membrane. When membranes had to be connected with each other forming a membrane block, it was done by connecting stiffening disks of successive membranes. A stiffening disk placed on a membrane was also used as a throttle plate.

Stiffening disks had two disadvantages though. First, they increased diameters of membranes since their stiffened part did not participate in flexions, and consequently it resulted in the increase of a diameter of the whole device. Second, a stiffening disk added its own mass to the mass of a membrane, strongly lowering self- oscillation frequency. With a membrane block, the mass of stiffly connected stiffening disks deteriorated still more the dynamic properties.

In order to avoid that disadvantageous influence it was decided to do without a block of stiffly connected membranes.

It has resulted in using exclusively free membranes, i.e. fastened only on their edge and not connected mechanically with anything in their central part.

Introduction of the principle of free membranes brought about, when compared to membranes with stiffening disks, a marked decrease of diameters of logical elements and the improvement of dynamic properties.

As presented below, this principle imposed a kind of logical functions which may be realized by so designed pneumatic logical elements.

4. The principle of feed-back force from supply air

In membrane pneumatic logical elements, when input signals disappear an element should come back to its former state; on the other hand, the appearance of input signals should switch an element, /i.e. change its output signal for a second of the two values which this signal may take/, when those input signals exceed a definite pressure value, called a switching value.

For this purpose some designs apply support pressure, having an intermediate value between the two values of a used binary signal or springy parts.

The above discussed principle of free membranes results in small dimensions and small movable masses thus, in designing, it permits to obtain an adequate feedback force in a logical element from the entering supply air coming into an element. This force is effected on properly shaped moving switching parts of an element.

The application of a feedback force from supply air allows to avoid springy parts which limit permitted number of actions of an element.

5. The principle of elimination of pneumatic resistance

Pneumatic resistance found a wide application in pneumatic analogue control, being used mainly to form pneumatic cascades.
Then is has become to be applied together with a cascade in some designs of discreet control.

In discreet control however it is possible to do without pneumatic resistance. It has the advantage of avoiding increased demands for quality of supply air. Pneumatic resistance should be periodically examined and cleaned. The principle of elimination of pneumatic resistance increases the reliability of control.

6. The design of elements

It is known from the theory of logical systems that there is a number of full systems of logical elements, i.e. such sets of basic elements from which any complex logical system can be built.

For a given complex logical system the minimum possible number of elements used for its construction will be different depending on a chosen full system of basic elements. Sometimes it becomes advantageous to use a "over-stiffened" system, i.e. when any additional element is added to a full

system, what however increases the number of basic elements, but at the same time mostly facilitates the synthesis of complex systems and decreases the total number of the used elements.

It might be possible for a group of applications, when examining their logical systems, to search such a full or "over-stiffened" system which would offer the minimum wear of basic elements to construct a given kind of systems. Another way of searching an optimum set of basic elements is made by designing such elements, when the design imposes generally the kind of logical functions which can be realized by those elements. Then the search is made among those functions to find a full or "over-stiffened" system.

The second way was chosen, and the design /Fig. 1,2,3 and 4/ was conditionned by the above discussed three principles, i.e. the principle of free membranes, the principle of feedback force and the principle of elimination of pneumatic resistance.

Fig. 1 shows three membranes placed freely in a shell. The shape of a shell and the position of free, flat membranes are responsible for the fact that the membrane beneath the chamber where pressure is introduced strains downwards; but the membrane in the chamber itself only adjoins against the shell which is over it.

If now pushers not connected mechanically with anything else, as shown in Fig. 2, are placed among free membranes, then bringing pressure to any chamber will always cause the strain downwards of the lowest membrane. The strain will appear also when pressure is brought to some, or even to all the chambers simultaneously.

Fig. 3 and 4 show the principle of action of the lowest membrane on a switching plate nad a pusher. Fig. 3 presents a solution for an OR-function, and Fig. 4 for a NOR-function. Each of those figures show two states, and namely, the state "a" /Fig. 3a and 4a/, when the lowest membrane remains without strain, and a switching plate by the feedback force from supply air switches a switching set into its higher position, and the state "b" /Fig. 3b and 4b/, when the lowest membrane

is strained by force which has exceeded the feedback force and switched a switching set into its low position.

Since the strain of the lowest membrane is connected through an OR-function with the appearance of pressure in individual chambers of free membranes, it is evident that Fig. 3 presents a switching set of an OR-element, because together with the strain of the lowest free membrane there appears the free supply pressure on the output. Consequently Fig. 4 presents a NOR-element, since with the strain of the lowest free membrane the output is connected to atmosphere.

As presented in Fig. 3 and 4, the output channel of an element, when not being connected to supply air, is connected to atmosphere, which secures de-aeration of signal line in passing from a binary state "1" to a binary state "0".

7. Assembling an element

For technological reasons the construction was restricted to four-input elements. All parts of an element /Fig. 5a/ are placed quite loosely into a cylinder, without any mechanical connections.

Establishing position of individual parts of an element is made possible by the stripes of membranes 7 and the seal 8 inserted in appropriate holes of the bed 1, of the segment 2, of distance rings 3 and the cap 4.

The moving parts, such as the pusher 6, the switching plate 9 and the intermediate pushers 5 move freely within chambers of individual rings. Connecting individual chambers to an appropriate channel, one of the four placed at 90° channels of the input signals, is made possible by radial passages in the distance rings 3 and the cap 4. Those rings are turned properly during assembling and they connect a chamber to an appropriate channel. All individual internal parts are fixed by pressing only the closing cap 4 into the cylinder 10, and then the bed 1 leans against a lower stripe of the cylinder /Fig. 5a and 5b/.

The closing cap is being pressed until individual chambers are completely tight, and the switching set operates smoothly.

An element is assembled on an assembling stand, what facilitates a quick controlling of tested parameters. Thanks to the presented design and the way of assembling it is possible to introduce a full assembling automation on an specially designed stand.
Elements of OR-function and NOR-function are assembled mostly of identical parts. There is only one difference in design between the two kinds of elements. It consists of different dimensions of the bed 1 and the pusher 6, and in the 180° difference in turning of the segment 2.

8. Used materials

Individual parts of an element can be made of different materials and by different methods depending on maker's possibilities and the requirements of exploitation.

It seems extremely advantageous to form parts of an element by means of a pressing technique. There are two methods of forming parts, and namely, of metal, or of pressed plastic material which reaches its final state by a thermal treatment. Elastic parts are made of oil-proof rubber within the temperature range of -50° Cent. and +120° Cent., what covers practically the whole range of needed temperatures.

There are tests being made in order to replace rubber by a more suitable material.

9. Realized logical functions

It may be concluded from the above described switching process of elements that their basic types realize OR-, or NOR-functions.

$$y = x_1 + x_2 + x_3 + x_4 \qquad /1/$$

$$y = \overline{x_1 + x_2 + x_3 + x_4}.$$

Using air supply chanel to bring an additional input

signal x_0 makes possible to realize the following functions

$$y = x_0/x_1 + x_2 + x_3 + x_4/ \qquad /2/$$

$$y = x_0/\overline{x_1 + x_2 + x_3 + x_4}/$$

The fact that both types of elements can be made as four-, three-, two-, or one-input, allows to realize all particular cases of the given equations.

In the case when a supply channel is not used for an additional signał x_0, elements have a signal "1" taken directly from supply. In such a case they are called "active" elements.

An output "0" signal is always obtained by direct connection of output to atmosphere.

10. Some technical data

The elements made for testing purposes in the Chair of Mechanical Automatic Control at the Technical University of Warsaw were of aluminium yet, and not of a plastic material.

Their technical data are as follows:

supply pressure	$p_s = 100 \div 140$ KN/m^2
pressure of signal "1"	$0{,}8 \div 1{,}0\ p_s$
pressure of signal "0"	$0 \div 0{,}2\ p_s$
overload pressure	200 KN/m^2
flow /when Δp = 100 KN/m^2/	$Q \cong 0{,}28$ dm^3/s

external dimensions and weights of cylindrically shaped elements

one-input element	Ø 20 x 12 mm	0,10 N
two-input element	Ø 20 x 15 mm	0,12 N
three-input element	Ø 20 x 18 mm	0,14 N
four-input element	Ø 20 x 21 mm	0,15 N

tested switching number of an element 10^8

11. Laboratory tests of static properties

If pneumatic logical elements with moving parts are "active" elements, they, as it is generally known, have practically unlimited logical amplification.

Investigating a number of systems built of the above presented elements, even of AND-function /which are semi-passive elements/, no difficulties were encountered with unsufficient logical amplification.

The next, after logical amplification, and the essential static property of pneumatic logical elements, is their switching zone.

Laboratory tests have pointed out that between a switching zone and the zones of tolerance of signals "0" and "1" there are tightening zones, which cannot be included to zones of tolerance of signals. That is due only to the fact that within a tightening zone air leakage is too high for steady states.

The typical results of laboratory tests of static characteristic of repetition element are presented in Fig. 6. Hysteresis loop consisting of two switching branches, from "0" to "1", and from "1" to "0", might be different in different elements, and it is differently placed. Those factors are without any importance if the hysteresis loop is placed within a switching zone, yet /zone c, Fig. 6/.

On account of the use of supply air in steady states tolerance zones of signals /zones a and c, Fig. 6/, and tightening zones /zone c, Fig. 6/ should be distinguished. If this distingushing is not necessary, tightening zones may be then regarded as an anlargment of tolerance zones of signals. In this case signal tolerance becomes 30 per cent.

12. Experimental determination of dynamic properties

Dynamic properties of an element of repetition were presented in Fig. 7 in the form of a step-function response calculated from the results of laboratory tests.

It is difficult to obtain a step function response directly from an experiment. An indirect measurement was made

in this way, that giving on input the same step function several times, the times between the appearance on input and output of the same pressure were measured. So obtained times for different pressure values were used as abscissa of a step function response. In this way the imperpection of the realization of a step function was partially corrected.

As show in Fig. 7 the total time of switching is below 2,5 mil. sec.

Dynamic tests of multi-input elements and the apropriate theoretical considerations have not come to an end, yet.

Literature

1. Jacewicz Jan, Olszewski Mariusz: "Pneumatyczne membranowe elementy logiczne", Pomiary Automatyka Kontrola 1966 r. nr 6 str. 196 - 200.
2. Jacewicz Jan, Olszewski Mariusz: "Projekt części centralnej membranowej systemu MERALOG" - Materiały IV Krajowej Konferencji Automatyki Kraków 1967 r. tom VI str. 87 - 98.
3. Leśkiewicz Henryk J.: "A Cascade Jet Logical Element" Proceedings of the Third Congress of the International Federation of Automatic Control, London 1966, p.p.31 C.1-3.
4. Leśkiewicz Henryk J., Żelazny Marek: "Koncepcja systemu dyskretnych płynowych elementów automatyki MERALOG" - Materiały IV Krajowej Konferencji Automatyki, Kraków 1967 r. tom VI str. 157 - 168.
5. Leśkiewicz H.J., Kaczanowski S., Kościelny W.: "Construction of Logic Systems from four-, three-, and two- input Cascade Jet Fluidics" - Proceedings of the Third Cranfield Fluidics Conference, Turin 1968.
6. Tal A.A.: "Realization of Sequential Machines by Means of Pneumatic Automation" - Proceedings of the Third Congress of the International Federation of Automatic Control, Basel, Switzerland 1963, str. 593 - 602.
7. Töpfer H., Schrepel D., Schwartz A.: "Universelles Baukastensystem für pneumatische Steuerungen" - Messen. Steuern. Regeln. 1964, nr 2, str. 63 - 72.
8. Töpfer H., Schrepel D., Schwartz A.: "Pneumatische Steuerungen" Berlin 1967.

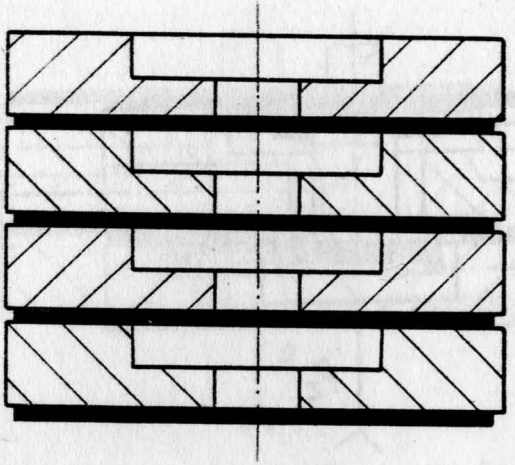

Fig. 1. Undeflected free membranes in schells.

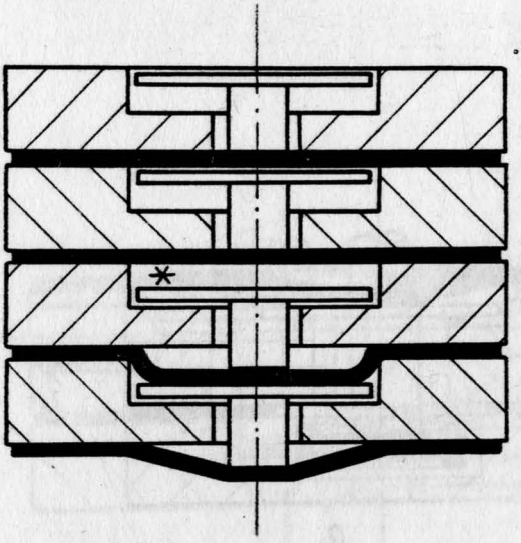

Fig. 2. Deflection of free membranes with free pushers by pressure in a chamber /marked with an asterisk/.

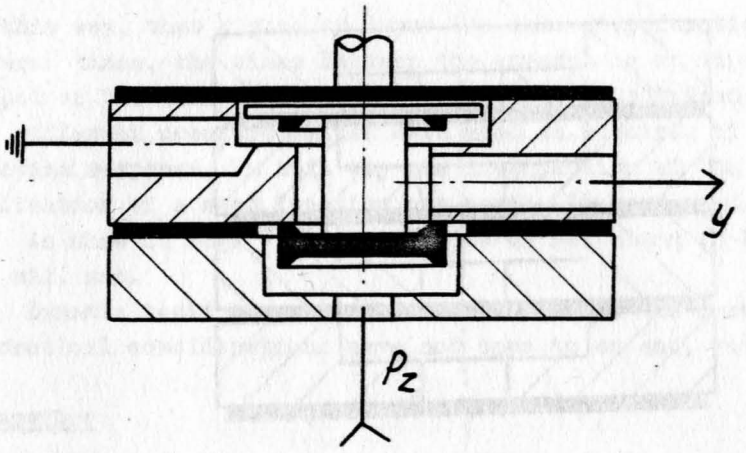

Fig. 3a. Switching system of an OR-element by an undeflected lowest free membrane.

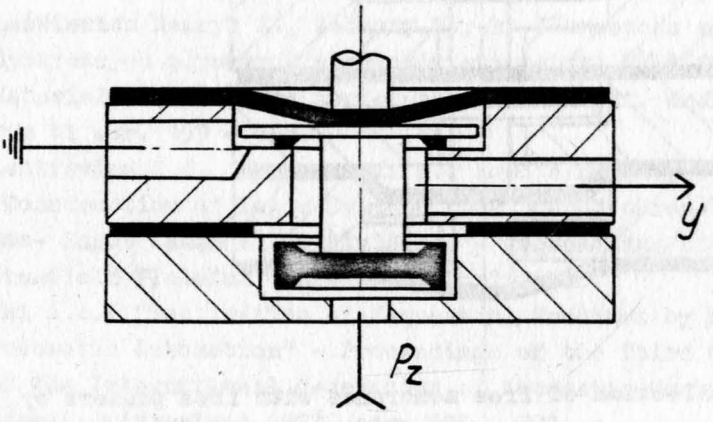

Fig. 3b. Switching system of an OR-element by a deflected lowest free membrane.

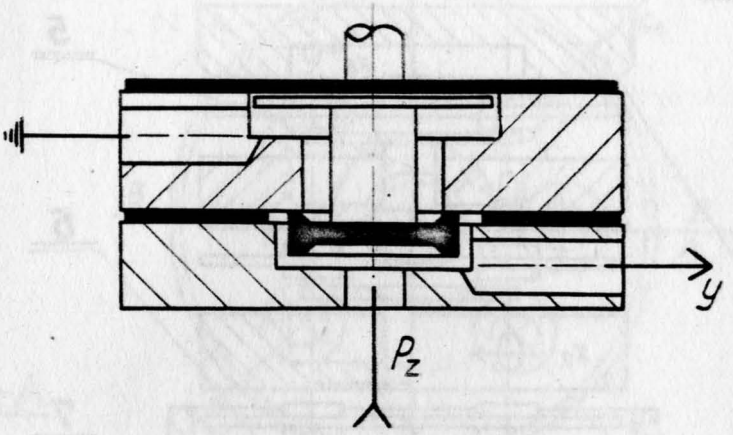

Fig. 4a. Switching system of a NOR-element by an undeflected lowest free membrane.

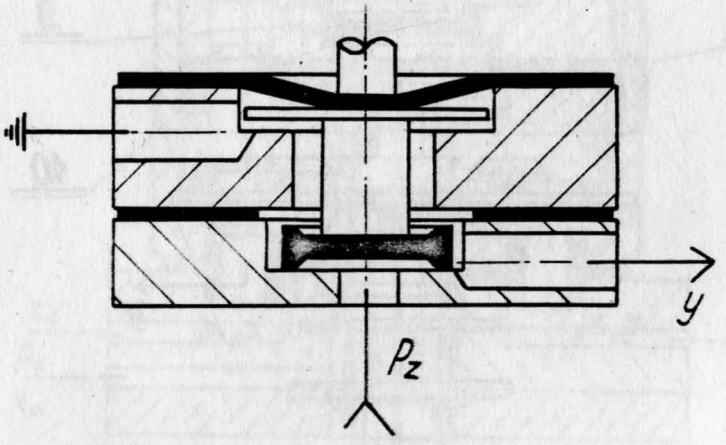

Fig. 4b. Switching system of a NOR-element by a deflected lowest free membrane.

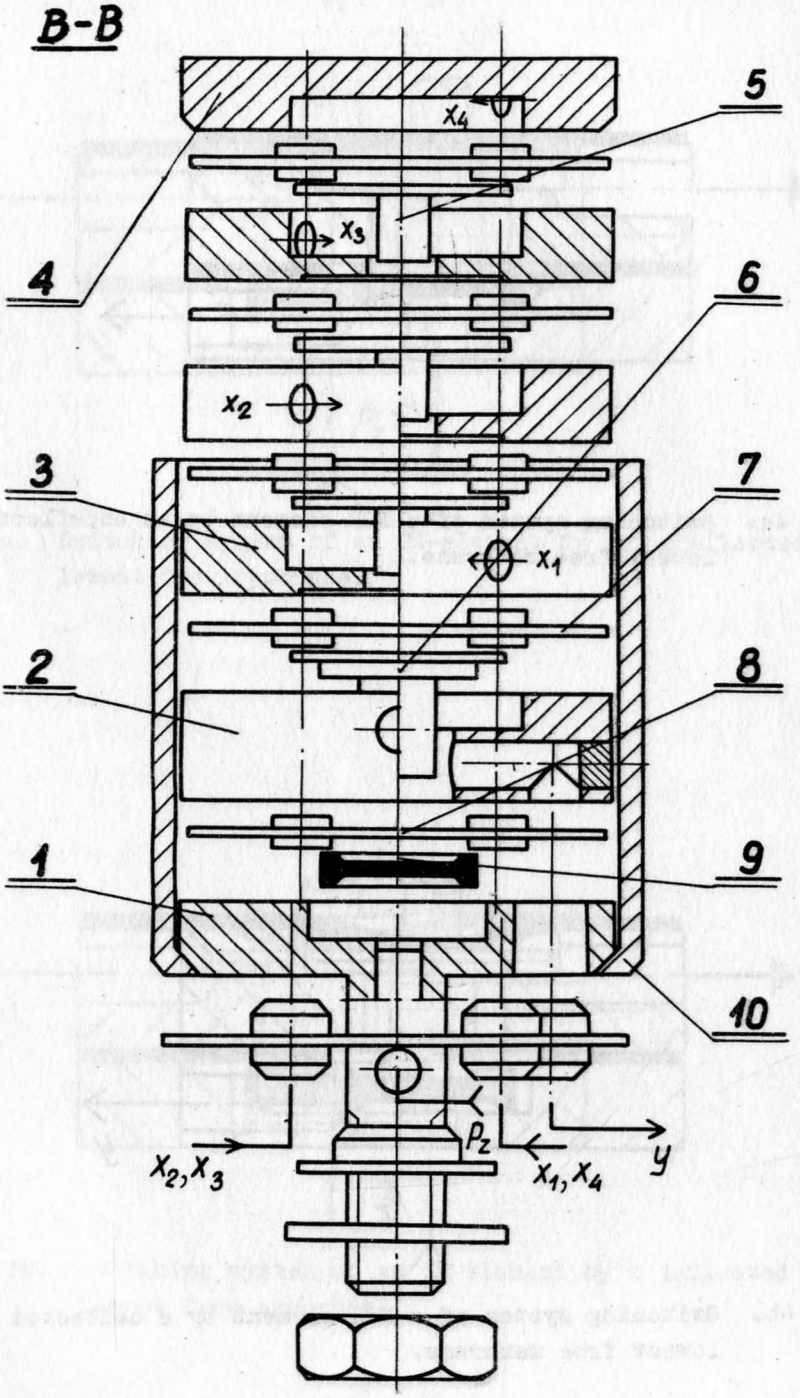

Fig. 5a. An OR-element while being assembled.

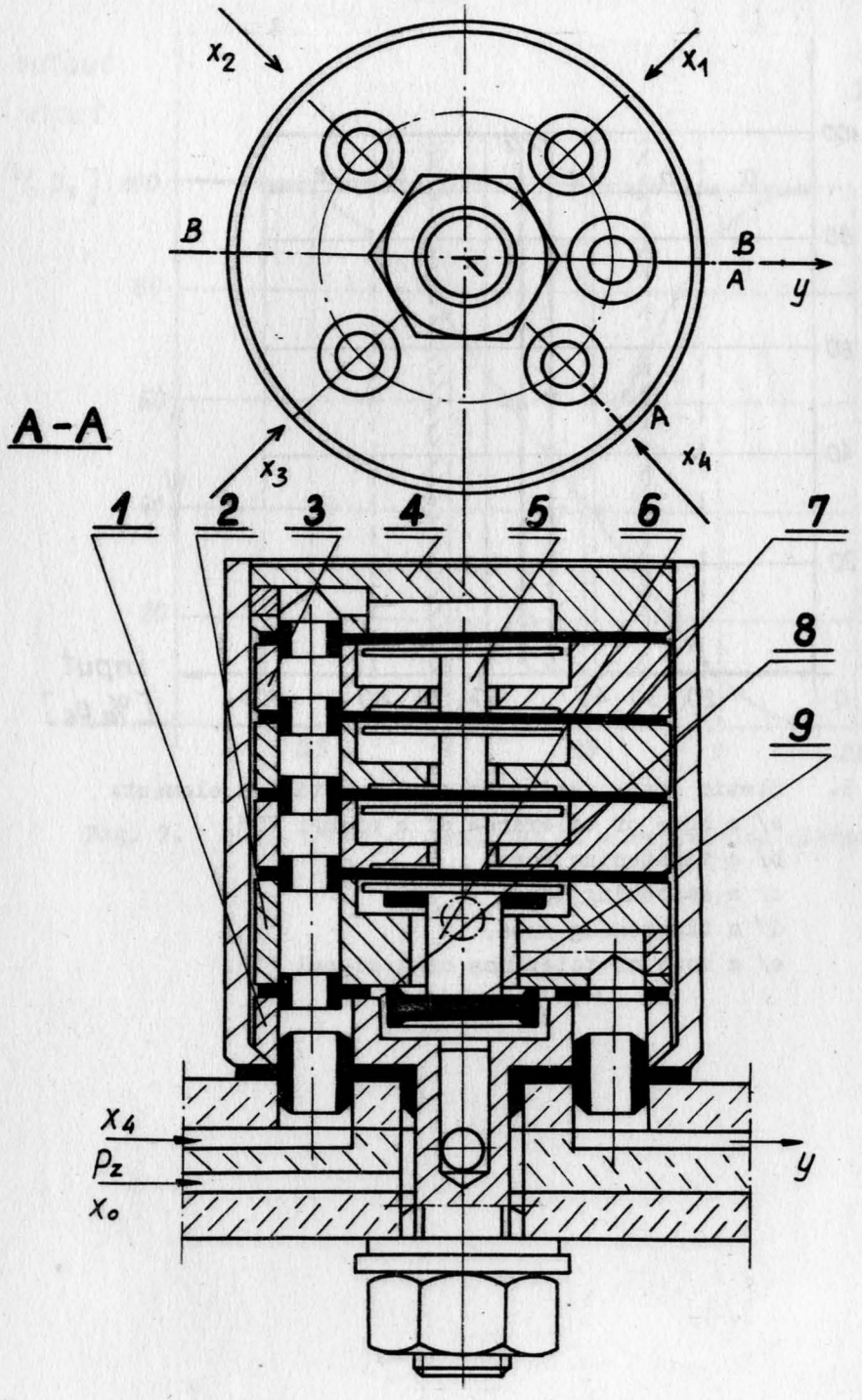

Fig. 5b. An assembled OR-element.

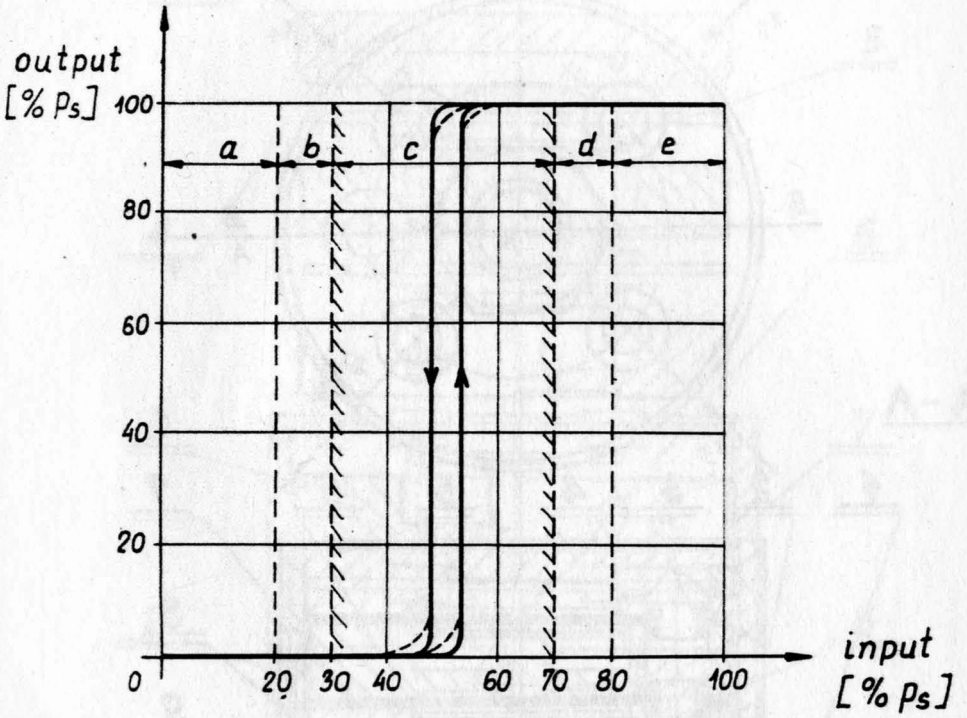

Fig. 6. Static characteristics of a repetition element:
a/ a zone of tolerance of a signal "0",
b/ a tightening zone,
c/ a switching zone,
d/ a tightening zone,
e/ a zone of tolerance of a signal "1".

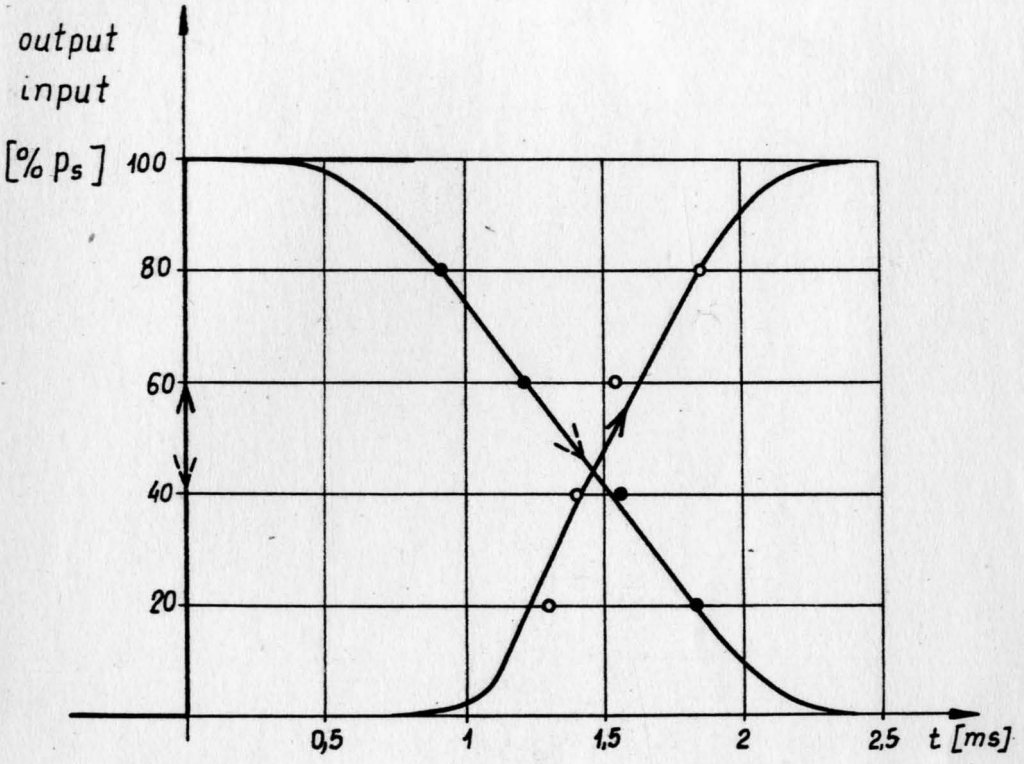

Fig. 7. Step function response of a repetition element.